AD-777 087

SURFACE INTERACTIONS AND LUBRICATION RESPONSE OF SILICON NITRIDE BEARING ELEMENTS

H. Dalal, et al

SKF Industries, Incorporated

Prepared for:

Naval Air Systems Command

February 1974

AD777087

FINAL REPORT

ON

SURFACE INTERACTIONS AND LUBRICATION RESPONSE OF SILICON NITRIDE BEARING ELEMENTS

February, 1974

Contributors

H. Dalal
Y. P. Chiu
J. I. McCool
O. G. Gustafsson

Prepared: Harish M Dalal

Approved:

Released:

U.S. Navy Contract No. N00019-73-C-0150
SKF Report AL74P009
SKF Code LC136
SKF Reg. 414 2

SUBMITTED TO:

U.S. DEPARTMENT OF THE NAVY
NAVAL AIR SYSTEMS COMMAND
CODE AIR 310C (JP1)
WASHINGTON, D.C. 20360

RESEARCH LABORATORY
SKF INDUSTRIES, INC.
ENGINEERING AND RESEARCH CENTER
KING OF PRUSSIA, PA.

UNCLASSIFIED

Security Classification

DOCUMENT CONTROL DATA - R&D

(Security classification of title, body of abstract and indexing annotation must be entered when the overall report is classified)

1 ORIGINATING ACTIVITY (Corporate author) SKF Industries, Inc. Research Laboratory Technology Services Center King of Prussia, Pennsylvania	2a REPORT SECURITY CLASSIFICATION Unclassified 2b GROUP

3 REPORT TITLE

Surface Interactions and Lubrication Response of Silicon Nitride Bearing Elements

4 DESCRIPTIVE NOTES (Type of report and inclusive dates)

Final Report

5 AUTHOR(S) (Last name, first name, initial)

H. Dalal, Y. P. Chiu and J. I. McCool

APPROVED FOR PUBLIC RELEASE; DISTRIBUTION UNLIMITED

6 REPORT DATE	7a. TOTAL NO. OF PAGES	7b. NO. OF REFS
February, 1974	108	25

8a. CONTRACT OR GRANT NO. Contract No. N00019-73-C-0150	9a. ORIGINATOR'S REPORT NUMBER(S) AL74P009
b. PROJECT NO. NEW	
c	9b OTHER REPORT NO(S) (Any other numbers that may be assigned this report)
d	

10 AVAILABILITY/LIMITATION NOTICES

~~Qualified requestors may obtain copies of this report from DDC~~

11 SUPPLEMENTARY NOTES	12. SPONSORING MILITARY ACTIVITY Department of the Navy Naval Air Systems Command

13 ABSTRACT

This is the Final Report summarizing results of a fundamental investigation of the suitability of silicon nitride as a rolling bearing material with emphasis on its interactive behavior with lubricating fluids.

The need for a light-weight bearing material in critical high-speed turbine applications is discussed and the potential benefits of silicon nitride in particular are reviewed. The wettability characteristics of six lubricants on a silicon nitride surface were measured to determine which lubricants are apt to be successful with silicon nitride bearing components in permitting the replenishment of lubricant onto the rolled-over tracks which is vital for the maintenance of an elastohydrodynamic (EHD) film and the consequent prevention of surface initiated fatigue.

Lubricant film thickness and traction force were measured with an SKF optical EHD apparatus. Friction and wear studies were conducted under subcontract by Prof. E. Rabinowicz of M.I.T. Seven endurance tests were run at SKF using different combinations of tool steel rollers and steel or Si_3N_4 flats.

DD FORM 1 JAN 64 1473

Security Classification

UNCLASSIFIED

Security Classification

14 KEY WORDS	LINK A ROLE	LINK A WT	LINK B ROLE	LINK B WT	LINK C ROLE	LINK C WT
Silicon Nitride						
Rolling Contacts						
Elastohydrodynamic Lubrication						
Lubricants						
Optical Interference						

INSTRUCTIONS

1. ORIGINATING ACTIVITY: Enter the name and address of the contractor, subcontractor, grantee, Department of Defense activity or other organization (*corporate author*) issuing the report.

2a. REPORT SECURITY CLASSIFICATION: Enter the overall security classification of the report. Indicate whether "Restricted Data" is included. Marking is to be in accordance with appropriate security regulations.

2b. GROUP: Automatic downgrading is specified in DoD Directive 5200.10 and Armed Forces Industrial Manual. Enter the group number. Also, when applicable, show that optional markings have been used for Group 3 and Group 4 as authorized.

3. REPORT TITLE: Enter the complete report title in all capital letters. Titles in all cases should be unclassified. If a meaningful title cannot be selected without classification, show title classification in all capitals in parenthesis immediately following the title.

4. DESCRIPTIVE NOTES: If appropriate, enter the type of report, e.g., interim, progress, summary, annual, or final. Give the inclusive dates when a specific reporting period is covered.

5. AUTHOR(S): Enter the name(s) of author(s) as shown on or in the report. Enter last name, first name, middle initial. If military, show rank and branch of service. The name of the principal author is an absolute minimum requirement.

6. REPORT DATE: Enter the date of the report as day, month, year, or month, year. If more than one date appears on the report, use date of publication.

7a. TOTAL NUMBER OF PAGES: The total page count should follow normal pagination procedures, i.e., enter the number of pages containing information.

7b. NUMBER OF REFERENCES: Enter the total number of references cited in the report.

8a. CONTRACT OR GRANT NUMBER: If appropriate, enter the applicable number of the contract or grant under which the report was written.

8b, 8c, & 8d. PROJECT NUMBER: Enter the appropriate military department identification, such as project number, subproject number, system numbers, task number, etc.

9a. ORIGINATOR'S REPORT NUMBER(S): Enter the official report number by which the document will be identified and controlled by the originating activity. This number must be unique to this report.

9b. OTHER REPORT NUMBER(S): If the report has been assigned any other report numbers (*either by the originator or by the sponsor*), also enter this number(s).

10. AVAILABILITY/LIMITATION NOTICES: Enter any limitations on further dissemination of the report, other than those imposed by security classification, using standard statements such as:

(1) "Qualified requesters may obtain copies of this report from DDC."

(2) "Foreign announcement and dissemination of this report by DDC is not authorized."

(3) "U. S. Government agencies may obtain copies of this report directly from DDC. Other qualified DDC users shall request through
_______________________________."

(4) "U. S. military agencies may obtain copies of this report directly from DDC. Other qualified users shall request through
_______________________________."

(5) "All distribution of this report is controlled. Qualified DDC users shall request through
_______________________________."

If the report has been furnished to the Office of Technical Services, Department of Commerce, for sale to the public, indicate this fact and enter the price, if known.

11. SUPPLEMENTARY NOTES: Use for additional explanatory notes.

12. SPONSORING MILITARY ACTIVITY: Enter the name of the departmental project office or laboratory sponsoring (*paying for*) the research and development. Include address.

13. ABSTRACT: Enter an abstract giving a brief and factual summary of the document indicative of the report, even though it may also appear elsewhere in the body of the technical report. If additional space is required, a continuation sheet shall be attached.

It is highly desirable that the abstract of classified reports be unclassified. Each paragraph of the abstract shall end with an indication of the military security classification of the information in the paragraph, represented as *(TS)*, *(S)*, *(C)*, or *(U)*.

There is no limitation on the length of the abstract. However, the suggested length is from 150 to 225 words.

14. KEY WORDS: Key words are technically meaningful terms or short phrases that characterize a report and may be used as index entries for cataloging the report. Key words must be selected so that no security classification is required. Identifiers, such as equipment model designation, trade name, military project code name, geographic location, may be used as key words but will be followed by an indication of technical context. The assignment of links, rules, and weights is optional.

if

Security Classification

TABLE OF CONTENTS

TABLE OF CONTENTS (CONTINUED)

LIST OF ENCLOSURES

LIST OF ENCLOSURES (CONTINUED)

LIST OF ENCLOSURE (CONTINUED)

AL74P009

SURFACE INTERACTIONS AND LUBRICATION RESPONSE OF SILICON NITRIDE BEARING ELEMENTS

1. SUMMARY

This is the Final Report summarizing progress from November, 1972, through November, 1973, on a fundamental investigation conducted under Contract N00019-73-C-0150, of the suitability of silicon nitride as a rolling bearing material with emphasis on its interactive behavior with lubricating fluids.

This report contains the following sections:

Background. The need for a light-weight bearing material in critical high-speed turbine applications is discussed and the potential benefits of silicon nitride in particular is reviewed. There follows a discussion of the methods in use for producing silicon nitride, and a listing of the various physical properties of the hot pressed silicon nitride used in this program.

Wettability. The equipment and procedure, which were used to study the wettability characteristics of six lubricants against a silicon nitride surface, are described. These studies were made to determine which lubricants are apt to be successful with silicon nitride bearing components in permitting the replenishment of lubricant onto the rolled-over tracks which is vital for the maintenance of an elastohydrodynamic (EHD) film and the consequent prevention of surface initiated fatigue. The contact angle between the fluid and solid surface was used as an indicator of the wettability. The six lubricants used were: (1) Two synthetic paraffinic hydrocarbons with and without additions, (2) two ester oils with and without additions, (3) a mineral oil and (4) a polyphenyl ether.

Optical EHD Studies. A test rig developed by SKF for measurement of lubricant film thickness and traction force in elastohydrodynamic contacts of a ball or roller and a glass flat is described. The same six lubricants, that were used in the wettability study, were tested with the optical EHD apparatus. Fringe photographs of the contacts between a transparent glass flat and silicon nitride balls were obtained. In order to obtain clearly visible fringes the optical properties of the test element (1/2 inch diameter silicon nitride ball) and those of the

coating of the glass flat must be well matched. The optimum reflectivity of the coating of the glass flat was determined theoretically and confirmed experimentally. Suitable coatings were selected. A series of fringe photographs were obtained on the optical EHD tester at two loads and rolling velocities in the 5 to 400 inch/sec. range with Si_3N_4 - glass contacts.

Traction Tests. The optical EHD rig was also used to measure the traction force at the contact between the flat and the ball, each of which is connected to a driving spindle. The sliding rate is defined as the difference in surface speed of the two bodies. Tests were run to determine the traction coefficient as a function of sliding and rolling velocity, for the six test oils. Data were obtained for steel/steel, steel/silicon nitride and glass/silicon nitride contacts.

Sliding Friction and Wear Studies. A two-dimensional statistical description of a rough surface based on a paper written by Longuet-Higgins was presented and applied to the surface of a ground silicon nitride plate for comparison with similar measurements on ground steel surfaces. Friction and wear studies were conducted under subcontract by Professor E. Rabinowicz of MIT. In these tests a "pin on disk" apparatus was used. The top specimen is a 1/4 inch diameter rod which was pressed against the bottom specimen, a plate rotated at a speed of 0.3 cm/sec in the friction tests and 30 cm/sec. in the wear tests. A "Lapmaster" abrasive wear test apparatus was also used in some tests.

Flat Washer Surface Interaction Studies. The flat washer tester contains three rollers, guided by a plastic or metal cage, and rolling under load between two flat washers. In the tests under the present contract, the rollers were made of M50 or Rex 49 tool steel, the top washer was made of 52100 steel and the bottom washer of silicon nitride or 52100 steel. Seven endurance tests were run using different combinations of rollers and flats with an ester-base lubricant.

2. CONCLUSIONS

1. There are considerable differences between the wetting behavior of the six test lubricants against a silicon nitride surface. The contact angle varies from 5° (for Mobil DTE Medium Heavy Mineral Oil) to 37° (for the five-ring polyphenyl ether OS124). The lowest contact angles were obtained with the DTE Medium Heavy oil and the Mobil Jet II. The contact angle was found to be larger in the direction perpendicular to the surface lay than parallel to it (for the same surface roughness in both directions). The lubricants, with one exception, give smaller contact angles for a smoother surface (1.5 μin CLA surface roughness) than for a rougher surface (15 μ inch CLA surface roughness).

2. The optical EHD test rig at SKF was found to be suitable for film thickness studies using silicon nitride/glass contacts. CeO and SiO coatings on the glass flat with a reflectivity of approximately 25% were found theoretically and experimentally, to give optimum results.

3. The plateau film thickness measured from the fringe photographs, at two loads and 9 rolling velocities in the 5-400 in/sec range is smaller for the silicon nitride contact than for the steel contact by 15 to 20%. The computed film thickness overestimates the measured film at high velocities.

4. A study of the oil meniscus lines (indicating partial EHD starvation conditions) in the fringe photographs of steel-glass and silicon nitride-glass contacts shows that the steel-glass contact is somewhat less starved than the silicon nitride contact, especially at higher speeds. Nevertheless, the fringe photographs indicate that the silicon nitride contact has satisfactory film building behavior close to what is expected by current EHD theory.

5. The traction coefficient in a silicon nitride/glass contact was found to rise with <u>sliding</u> speed and then level off, as in previous tests with steel contacts. This shape of the curve was typical for 4 of the 6 oils tested. The other two curves reached a maximum and then decreased with <u>sliding</u> speed Test data also showed that the traction coefficient increases with load but decreases with <u>rolling</u> speed, a trend which is consistent with previous traction tests in steel contacts. The effect on traction of additives in paraffinic and ester oils is small.

2. CONCLUSIONS

1. There are considerable differences between the wetting behavior of the six test lubricants against a silicon nitride surface. The contact angle varies from 5° (for Mobil DTE Medium Heavy Mineral Oil) to 37° (for the five-ring polyphenyl ether OS124). The lowest contact angles were obtained with the DTE Medium Heavy oil and the Mobil Jet II. The contact angle was found to be larger in the direction perpendicular to the surface lay than parallel to it (for the same surface roughness in both directions). The lubricants, with one exception, give smaller contact angles for a smoother surface (1.5 μin CLA surface roughness) than for a rougher surface (15 μ inch CLA surface roughness).

2. The optical EHD test rig at SKF was found to be suitable for film thickness studies using silicon nitride/glass contacts. CeO and SiO coatings on the glass flat with a reflectivity of approximately 25% were found theoretically and experimentally, to give optimum results.

3. The plateau film thickness measured from the fringe photographs, at two loads and 9 rolling velocities in the 5-400 in/sec range is smaller for the silicon nitride contact than for the steel contact by 15 to 20%. The computed film thickness overestimates the measured film at high velocities.

4. A study of the oil meniscus lines (indicating partial EHD starvation conditions) in the fringe photographs of steel-glass and silicon nitride-glass contacts shows that the steel-glass contact is somewhat less starved than the silicon nitride contact, especially at higher speeds. Nevertheless, the fringe photographs indicate that the silicon nitride contact has satisfactory film building behavior close to what is expected by current EHD theory.

5. The traction coefficient in a silicon nitride/glass contact was found to rise with <u>sliding</u> speed and then level off, as in previous tests with steel contacts. This shape of the curve was typical for 4 of the 6 oils tested. The other two curves reached a maximum and then decreased with <u>sliding</u> speed Test data also showed that the traction coefficient increases with load but decreases with <u>rolling</u> speed, a trend which is consistent with previous traction tests in steel contacts. The effect on traction of additives in paraffinic and ester oils is small.

The two paraffinic oils give the lowest traction coefficients, while the mineral oil and the polyphenyl ether exhibit relatively high traction. Tests with steel/steel and steel/silicon nitride show that at the highest stress level, 271 ksi, the traction for the two types of contacts differ by no more than 8%. At lower stress levels, 216 and 247 ksi, the differences are larger, in one case by more than 20%. The traction coefficient in the silicon nitride contacts is generally lower than that prevailing in steel contacts.

6. Results of the "pin on disk" tests at MIT indicate that the friction coefficient on ground silicon nitride surfaces is lower when the pin traverses across the grinding grooves than when it runs parallel to the grooves. Teresso V78 and Turbojet 2380 lubricants gave the lowest friction coefficients with a slight margin. Some of the lubricants tested, and especially the silicone, give higher friction coefficients than the unlubricated conditions.

7. Tests on the "Lapmaster" abrasive wear test apparatus at MIT using 600 grit silicon carbide as abrasive showed that silicon nitride results in an order of magnitude greater abrasive wear coefficient than the three other ceramics tested. The wear resistance of silicon nitride under lubricated sliding contact (in the "pin-disk machine") is found to be somewhat higher than for M50 steel. The wear coefficient of 2.2×10^{-6} is reasonable for a lubricated sliding system involving non-metallic materials.

8. Wear debris collected from the Lapmaster wear tests was examined at SKF using a Scanning Electron Microscope. The SEM photograph of the debris shows the presence of faceted particles. This supports the contention of silicon nitride being brittle on the microscale, under the stresses created by lapping.

9. The very limited fatigue tests at SKF covered in this report, run with an ester lubricant in a heavily loaded roller/flat washer configuration, have produced much shorter lives than predicted, both in baseline runs of steel/steel and in runs of silicon nitride/steel. (Further tests not reported here, under slightly modified conditions, gave normal lives). In the tests covered here, all fatigue was at the rollers, but there was wear at silicon nitride washers. Effects of lubrication, stress level, slide/roll ratio and surface roughness on fatigue life of silicon nitride all require further study. However, the tests reported do show that silicon nitride does not undergo catastrophic failure under rolling contact conditions.

3. BACKGROUND

3.1 The Need for Ceramic Bearing Research

Enclosure 1 taken from (1)* shows the estimates of six aircraft engine manufacturers of the industry's requirements up until 1975. It is seen that future aircraft engine bearings are expected to operate at speeds of 3×10^6 DN (DN = bearing bore diameter in mm times shaft speed in rpm) and temperatures in excess of 700°F. These requirements will pose a great challenge to proper bearing lubrication and life expectancy.

The predominant force on the balls in high speed engine bearings is the centrifugal force which induces such high outer ring contact forces that bearing life is reduced drastically as engine bearing speeds increase. A substantial portion of this loss in contact fatigue life can be regained if light-weight balls are used. Reducing the weight of steel balls by making them hollow introduces substantial manufacturing problems, such as the difficulty in achieving sufficient accuracy of the hole location. Endurance testing of hollow ball bearings has shown that the ball failure mode changes from contact fatigue to bending fatigue producing much shorter lives. Solid balls of low density bearing materials therefore are preferred.

Recent advances in ceramics technology have overcome many of the factors which have militated against the use of these materials as rolling bearing elements, notably porosity and excessive brittleness. The low density of ceramics coupled with their stability and high hardness levels at elevated temperatures have long made them appear desirable for use in bearings operating at extreme conditions. It can be expected that the use of new, stronger ceramic materials will offer improvements in high temperature properties over steels, and due to low weight, be favorable where centrifugal loading is critical.

*Numbers in parentheses refer to List of References at the end of this report.

It has only been recently however, that ceramic materials have been developed which show signs that the problems of brittleness and poor fatigue properties have been overcome to the degree required for reliable, long-lived rolling bearings. One such material is a new silicon nitride ceramic as currently made by the Norton Co. under a license from the U. K., and it is projected that bearings or bearing parts such as balls and rollers can be successfully made from this material.

The complex interactions that exist between bearing elements, surface finishing methods, lubricants and the environment prevent the direct extrapolation of performance of steel bearings, to bearings made of ceramic materials. Specifically, the elastic moduli of ceramics are significantly higher than those of steels, and, therefore, the use of standard bearing designs and loading practices would result in extremely high Hertzian stresses at the contacts. Certain tensile stresses in the Hertzian field may be critical in ceramic bearings instead of the Hertz shear stresses used in the design of steel bearings. Modified designs and loading rules will be required in order to reduce these stresses to an acceptable level. This acceptable level is unknown for ceramics. New designs will be required to resolve cooling of the bearings in view of the low thermal conductivity of ceramics.

3.2 The Importance of Surface Interaction and Lubrication Effects

Surface initiated spalling is a principal cause of failure in aircraft jet engine mainshaft ball and roller bearings (and many other types of rolling bearings). Surface initiated spalling has been observed to be critically dependent upon lubrication conditions and surface characteristics of the bearing materials (2).

Previous work under Contracts N00010-68-C-0310 and N00019-71-C-0425 have shown that there is a reduction of film thickness around the shoulder of surface furrows. Also, intimate surface contact can take place between asperities if there is insufficient lubricant film thickness. The existence of these microscopic imperfections prevents idealistic film profiles from being obtained in their vicinity. However, there is reason to believe that the severity of stress concentration at the micro-defect is influenced by both the lubricant film pressure and the bearing material strength and ductility characteristics. This stress concentration affects the surface fatigue life through its influence on the onset of surface distress (3).

In addition to the above lubrication-related bearing failure modes from surface defects, high-speed bearings sometimes suffer a type of surface failure known as skid damage which is distinctly different from the above-mentioned surface distress. Skid damage apparently is related to the occurrence of abrupt load changes in the presence of substantial sliding at the Hertzian contacts in bearings, and thus the occurrence of this damage can be influenced by the traction or sliding friction characteristic of the lubricant and bearing material interface as it affects the bearing kinematics.

The differences in response between ceramics and steels to manufacturing processes will undoubtedly produce new features of surface microtopography. These features will affect both the traction forces at the contacts and skidding and wear damage when surface asperities penetrate the EHD film. Additionally, the differences in surface chemistry between ceramics and steels suggest that the wetting behavior of lubricants, the response to boundary lubricant additives, and the susceptibility to stress corrosion cracking in chemically active environments will be significantly different. Finally, the fatigue and galling response of ceramics in Hertzian contacts is poorly understood and needs to be evaluated. All these novel problems support the need to conduct experiments into the behavior of ceramic materials in lubricated rolling contacts and to obtain the knowledge necessary to predict the behavior to be expected in full scale bearings.

3.3 Progress in the Application of Ceramics For Bearings

Early efforts at screening a wide variety of available ceramic materials for bearing applications met with only limited success due to the inherent porosity and lack of homogeneity of the then available materials (4,5). A comprehensive study of the application of ceramics technology to rolling bearings about ten years ago resulted in a bearing with the best available materials which gave remarkably promising performance (6). This bearing is illustrated in Enclosure 2 showing its good condition after successful operation at high speed (8000 rpm) and temperature (1500°F). This bearing was equipped with cemented carbide rings, ceramic balls and molybdenum cage and lubricated with MoS_2 powder in argon carrier and thrust loaded to 300,000 psi contact stress. Some deterioration of the contact surfaces in the raceway tracks was evident after this testing. These poor surface fatigue characteristics (presumably from poor structural integrity of the then currently available commercial compositions) have limited rolling-bearing use of ceramics.

F-4186A R100

The advantage of using ceramics for rolling bearing components stem from their following characteristics:

a) high strength and hardness at room as well as at elevated temperatures

b) low density

c) low material cost, and

d) excellent corrosion resistance.

The main disadvantages of ceramics are

a) brittleness,

b) high notch sensitivity,

c) low thermal conductivity, and

d) high finishing costs to accurate bearing tolerances.

The high modulus of elasticity of most ceramics results in high bearing stiffness but also in high contact stresses causing increasing severity of lubrication conditions.

Of the various ceramics tested for structural applications silicon nitride has shown the best performance (13, 14). It has out-performed other ceramics in terms of thermal shock resistance and resistance to wear. Silicon nitride therefore is an obvious candidate material for bearing applications.

Silicon nitride has two allotropic forms. The low temperature α -phase transforms to the high temperature β -phase between 2700°F and 2900°F. Both forms have a hexagonal crystal structure.

Structural components of Si_3N_4 can be manufactured in one of two ways.

a) Reaction Bonding: This method tends to leave 15-20% porosity in the part. It is, therefore, suitable only for the manufacture of stationary parts that are not subjected to high stresses or impacts.

b) Hot Pressing: Fully dense parts are produced by this method.

Rolling bearings require materials of construction which have superior performance characteristics from several different points of view. The desirable low density characteristics of silicon nitride must be complemented by other superior properties for it to become a viable rolling bearing material. The most essential properties for ball or roller and ring materials are

1. High hardness under operating conditions
2. Adequate contact fatigue strength
3. Adequate ductility
4. Adequate impact strength
5. Dimensional stability
6. Low friction and wear
7. Wettability by lubricants
8. Manufacturability to precise tolerances.

Properties of silicon nitride are compared with those of typical bearing steels in Enclosure 3. These properties have only recently been improved to the point where silicon nitride can be considered for use in rolling bearings. However, some properties, such as elastic modulus and thermal expansion coefficient, are sufficiently different from those of steel that modifications of standard bearing design practices will be required to utilize silicon nitride effectively in rolling bearings. Other properties, such as the high hardness, will require development of special manufacturing techniques to produce bearings. Some important properties of hot pressed silicon nitride produced by the Norton Co. are listed in Enclosure 4.

More details on the properties and manufacturing of silicon nitride specimens are given in the First Quarterly Report (8) on this contract.

To date very little is known about the behavior of Si_3N_4 in rolling contact. A few preliminary tests have been performed at NASA by Parker and Zaretsky (7). The tests were conducted in a five-ball tester under the following conditions:

Max. Hertz stress (psi)	800,000
Shaft speed (rpm)	9,400
Contact angle (degrees)	30
Race temperature (°F)	130

The above tests were performed on a group of 20 balls. The results of the tests are given below:

L_{10}, stress cycles	2.5×10^6
L_{50}, stress cycles	17×10^6
Weibull slope	0.99
Failure index	19 out of 20

A few of the spalled balls produced in the above tests were studied in a scanning electron microscope at SKF (see Enclosures 5 and 6. It is clear from Enclosure 5 that the morphology of the spalls on a Si_3N_4 ball is similar to those found on steel balls. Enclosure 6 shows a lubrication distress zone at the end of the spall. The severity of lubrication distress around the spall seems to be greater than that normally observed on steel balls.

The fatigue life of Si_3N_4 rolling elements has been found to be very sensitive to the processing technique used (23). Work at Norton has indicated that proper choice of processing steps can make a significant difference in the fatigue life of rolling elements. Enclosure 7 shows the surface of an unrun Si_3N_4 ball. The surface is seen to be pitted. The presence of such pits can cause a collapse of the lubricant film and lead to failure due to lubrication distress. It is therefore imperative that proper surface finishing techniques be found to exploit the full potential of Si_3N_4 for rolling contacts.

Other studies with the more advanced silicon nitride ceramics also have shown promising rolling contact fatigue life in element tests (23) with apparently some variability with surface condition and lubrication of the ceramic elements.

Principally under Navy contract, SKF has developed and operated an optical interferometric apparatus to define the parameters affecting elastohydrodynamic lubrication of ball and roller bearings. Theories of partial and full EHD behavior and of rolling contact fatigue have been developed and published by the SKF Laboratory (3, 15 and 17).

4. DETAILS

4.1 Wettability Study

One of the requirements for good lubrication and heat transfer is that the lubricant wet the bearing elements under all intended operating conditions. Oil wetting of ceramic surfaces is not as certain as with metal surfaces, and the wetting behavior of six specified oils on a silicon nitride specimen was therefore studied.

The six lubricants used in these tests consist of the following:

1. Mobil Jet II (Mil-L-23699)

This is Mobil Jet II as formulated with XRM 234 plus a proprietary additive package.

2. XRM 177F

The synthetic hydrocarbon designated XRM109F and described below has been modified by the addition of an additive package consisting of an oxidation inhibitor and anti-wear additive, to see what difference in surface properties may be induced by the use of these additives. This material is designated by the supplier (Mobil Oil Co.) as XRM 177F, and it has been tested extensively as a candidate advanced turbine engine mainshaft bearing lubricant.

3. DTE Medium Heavy

This is a conventional high quality Mobil turbine oil, refined from mineral oil and having added to it rust, oxidation and foam inhibitors. Its viscosity index is 95 and viscosities are 63.5 cs @ 100°F (295 SUS) and 8.2 cs @ 210°F (52.8 SUS).

4. XRM 109F

An unmodified synthetic hydrocarbon (paraffinic) which is made by polymerization of an alpha-decene. The particular material used is designated XRM 109F by Mobil. It has a viscosity of about 445 centistokes at 100°F and can be considered a quite pure fluid in the sense that the only constituents of the fluid are the products of the polymeric reaction with some removal of the light ends.

5. OS124

This is a five-ring polyphenylether which has a viscosity of about 35 centistokes at 100°F. Without an additive package, it is supplied by Monsanto Chemical Co. under the designation OS124, and it is the basestock for an advanced military turbine engine lubricant.

6. XRM 234

This chemical type of fluid tested is the base fluid of lubricants which are formulated to meet the specification MIL-L-23699 for aviation turbine engines. These fluids are mixed esters of polybasic and/or monobasic alcohols, the exact composition of which is generally proprietary with the particular supplier. The material selected for these studies is that which serves as the base of the Mobil Oil Co. product, Jet II. It has a viscosity of about 28 centistokes at 100°F.

A list of various properties of these six oils is given in Encl. 8.

The contact angle between the liquid surface and the solid specimen is commonly used as an indicator of the wettability of the liquid-solid interface.

An attempt was first made to use Adam and Jessop's (11) tilting plate method to measure the contact angle between the liquid surface and a silicon nitride specimen. This attempt did not, however, meet with much success due to the interference of the meniscus at the lubricant/glass interface on the sides of the container. Due to this interference, the angle between the plate and the oil surface cannot be clearly observed, making it difficult to obtain accurate and consistent readings. An Eberbach cathetometer was also tried without success. A modified drop method was finally used to obtain quantitative data on contact angles and is described below.

The procedure consists of projecting the shadow of a lubricant drop applied to the substrate, onto a photographic paper by means of a magnifying lens, developing the print, and measuring the contact angle of the image of the drop on the image of the plane surface of the substrate. Illustrative examples are shown in Encl. 9.

The plates were prepared by cleaning with a nonionic detergent and rinsed with water and acetone between each measurement.

The drops of oil, of approximately 0.01 mm dia., were delivered to the surface of the substrate from a fine hypodermic needle. The hypodermic needles and syringes were thoroughly cleaned before each use.

The drops of oil were carefully placed on the surface of the substrate and allowed to equilibrate for 30 seconds before projecting the image. After 30 seconds, the flow of the oil on the substrate appeared to stop and the image of the drop remained stable.

Two kinds of substrates were used for this investigation. A silicon nitride plate was surface ground to 15 microinch finish, having a uni-directional lay on the surface. The surface of the second silicon nitride plate substrate was diamond polished using 6 and 0.25 μm diamond paste successively. The surface thus produced had a roughness of 1.5 microinch with practically no directionality.

The flow of lubricant on the ground substrate was greater in the direction of the lay than across the lay, thus resulting in an oval drop as shown in more detail in the Second Quarterly Report (9). The oil flow was found to be uniform in all directions on the polished surface, resulting in a round drop.

The results of the measurements are shown in Encl. 10.

It appears from Encl. 10 that there are considerable differences in the wetting behavior of the lubricants tested. Mobil Jet II and the DTE Medium Heavy lubricants give the best overall wettability (the lowest contact angles).

Encl. 10 also shows that, in all cases except DTE Medium Heavy oil, the contact angle on the polished surface is lower than the highest reading obtained on the rougher surface.

4.2 Optical EHD Studies

4.2.1 Description of EHD Test Rig - Mechanical System

A test rig, developed by SKF for measurement of lubricant film thickness and traction force in a lubricated elastohydrodynamic (EHD) contact of a ball or roller and a glass flat, is described below.

The basic test configuration used in this study is shown in Encl. 11, and consists of the contact of a roller or 1/2" diameter ball and a rotating transparent disk. The optical system, situated above the disk, is used to photograph the interference fringes formed by lubricated contact between the ball and disk.

In order to control the rate of sliding between the roller or ball and the disk, the ball is driven by a quill through a flexible coupling, and the disk is connected to a vertical spindle. Figure (a) in Encl. 11 shows that the test ball is supported below by a disk which is actually a ring of a thrust ball bearing. The load is applied through this support bearing.

Figure (b) is a plan view of the test assembly. Three balls or rollers, equally spaced on a 1.5" pitch circle, are used to support the disk, one of the balls being the test ball. The test ball is restrained by a spring cage. The lateral force acting between the ball and cage is measured by a strain gage mounted on a leaf spring beam, and the torque in the driving quill is measured by a torque meter. The strain gage and torque sensor outputs are used to compute the traction in the contacts (15).

Encl. 12 is a photograph of the entire assembly. The device which loads the three balls (or rollers) against the transparent plate consists of a flexible diaphram, covering a cylinder into which controlled air pressure is introduced. The diaphram exerts a force on the lower thrust bearing washer, through an adapter. The load applied to the observed contact is controlled by means of a calibrated mercury manometer.

The test lubricant is gravity fed to the Teflon cage by a simple once-through system. The oil flow rate can be varied. The test lubricant temperature is measured by a thermocouple probe installed approximately 1/16" from the inlet of the contact.

Both the vertical and horizontal spindles are driven from one variable speed electric motor. A variable-ratio positive drive between the motor and the vertical spindle allows rolling with a controlled magnitude of sliding between ball or roller and plate. The degree of sliding can be changed if desired while viewing the contact.

4.2.2 Description of EHD Test Rig - Optical System

The layout of the optical system, consisting of microscope, light source and flats, is shown in Encl. 13.

Glass flats of high optical quality and low (0.2 μin rms) surface micro-finish were obtained. A high efficiency anti-reflective coating is applied to the upper surface of the glass flats giving approximately 0.2% reflectivity.

A high intensity pulsed Xenon lamp of short pulse duration (1.25-7 μ sec) is used as the light source for taking the fringe photographs. The maximum pulse rate is 1000 Hz, and the intensity of the lamp is 20-300 x 10^6 beam candles. An external capacitor is used in the circuitry to increase the lamp intensity to 10^9 beam candles and the pulse duration to 9 μ sec.

4.2.3 Test Lubricants

A total of six lubricants were selected for testing in the optical EHD rig. These are the same lubricants as those used in the wettability tests (Section 4.1). The oil trade names and their properties are listed in Encl. 8. Encl. 14 is an ASTM standard viscosity temperature chart for the six oils. As the chart shows, the oils cover a wide range of viscosities.

4.2.4 Film Measurement Techniques

The fringe photographs in Encl. 15 show typical contacts between a steel ball and the transparent plate under MIL-L-23699 lubricated conditions, consisting of a relatively flat plateau and a slender constriction at the back and side edges of the contact circle. The film thickness at the plateau varies with the operating and lubricant parameters. Because of the relative uniformity of the plateau film thickness, the fringegrams when viewed through the eye piece of the optical system, exhibit a dominant color which can be related to film thickness by means of a calibration process. The fringe order of the color can be readily identified by increasing the speed gradually from zero.

Encl. 16 is a calibration chart relating color to film thickness for a standard fluid (quinoline) with atmospheric pressure refractive index $n_o = 1.625$. For other fluids under high pressure having an effective refractive index n_p, the film thickness obtained from this calibration chart is multiplied by the factor $(1.625/n_p)$.

The refractive index of oil in a high pressure Hertzian contact (n_p) is greater than that measured at atmospheric pressure. The high pressure refractive index can be calculated using the Lorentz-Lorentz equation, together with hartung's equation for estimating density at high pressure. A computer program was used to calculate the effective refractive indices using ambient viscosity and atmospheric refractive index as input. The values of the refractive index of the six lubricants listed in Encl. 8 are plotted in Encl. 17 as a function of pressure.

4.2.5 Surface Preparation Studies

Twelve silicon nitride 1/2" diameter balls, manufactured by Industrial Tectonics, Inc. from Norton Grade 110 silicon nitride, were purchased for the optical elastohydrodynamic tests. Diameter and weight measurements on these balls yield a density of 3.17 g/cm^3, which is 99.7% of the theoretical density. These ball specimens were finished by the manufacturer, using an unidentified manufacturing process. Initial trial runs in the optical EHD apparatus demonstrated that the surface condition of the balls was such that no optical interference fringes could be observed. Scanning electron micrographs (Encl. 7) show that the surface is covered with pits of approximately one μm diameter, which are left by the final manufacturing operations.

The unusual appearance of the finished ball suggests that silicon nitride does not respond to manufacturing procedures in the same manner as steel (assuming that standard ball manufacturing procedures were used to produce the balls). It was reported (12) that silicon nitride specimens prepared by grinding with successively finer grit wheels, followed by lapping with diamond paste, had far greater fatigue life than specimens which were made by coarse grinding directly followed by diamond lapping, even though both specimens had the same surface finish. This information suggests that coarse grinding initiates microcracks in the surface, which can be removed by finer grinding, but that lapping does not remove sufficient material to eliminate the cracks. Such an interpretation implies that the silicon nitride surface is brittle on a microscale. Further evidence of microbrittleness is the pitted surface of the balls. Such pits can be produced if segments of material crack out of the surface during finishing processes. Experiments on lapping of silicon nitride by Professor Rabinowicz reveal that material removal under lapping with alumina abrasive occurs at a rate which is ten times faster than predicted by theory or occurs with other ceramics. One explanation for the faster lapping is that silicon nitride particles which are considerably larger than the abrasive particles are torn from the surface.

An attempt to produce a better silicon nitride surface than the one shown in Encl. 7 has been accomplished by polishing the surface by spinning the balls at high speed in a wood lap using ferric oxide as the abrasive. Scanning electron micrographs to determine the effect of this processing on surface texture are shown in Encl. 18. Optical interferograms with these balls show some weak colors which possibly can be used for EHD film thickness measurements. Encl. 19 is a black and white static fringe photograph of this silicon nitride ball contact showing a few interference fringes.

In order to obtain more clearly visible fringes than those shown in Encl. 19, the optical properties of the test element (1/2" diameter silicon nitride ball in the present case) and those of the coating on the glass flat must be well matched. In the case of a steel ball, a coating of cerium oxide with a reflectivity of 30% and absorption less than 1% is found to be adequate. Due to the lower reflectivity of the surface of the silicon nitride ball, a different coating must be used.

The intensities of light reflected from the surface of the silicon nitride ball and the coated (CeO with 30% reflectivity) glass flat are not well matched to produce clearly visible interference fringes.

Therefore, an investigation was made on the optical visibility of the contact considering reflectivity and absorption of the ball and various coatings.

The value of the reflectivity of the silicon nitride ball surface was obtained using a Pentax light-meter. A beam of light was reflected off the surface of a steel ball, and the intensity was measured on a relative scale on the light-meter to be 5.9. The steel ball was replaced with a silicon nitride ball, and the light-meter reading was found to be 5.3. According to the Pentax manual, the relationship between a pair of relative scale readings (r_1 and r_2) and the corresponding intensities I_1 and I_2 is as follows

$$\frac{I_1}{I_2} = 2^{(r_1-r_2)}$$

Since the reflectivity of steel ball surfaces in oil is known to be 60% (16), the reflectivity of the silicon nitride ball is calculated to be 44%.

In optical interferometry, the visibility of fringes is governed by the intensities of the two interfering light beams, (I_1 and I_2). In the optical system shown in Encl. 20, I_o is the intensity of the collinated beam from the objective lens. I_1 is the intensity of the beam reflected from the layer and I_2 is the intensity of the beam reflected back from the contact and through the coating (twice). The visibility is defined as the ratio of the geometric mean to the arithmetic mean of the two beam intensities I_1 and I_2 i.e. (16, 18)

$$V = 2(I_1 I_2)^{1/2}/(I_1+I_2)$$

Maximum visibility (V=1) occurs when $I_1 = I_2$.

Knowing the reflectivity and absorption coefficients of the layer and the ball, it is possible to compute the relative intensity of the two interfering beams I_1 and I_2 considering two ball materials (steel and silicon nitride) and various coating materials. Encl. 21 gives the properties of coatings investigated for this program as obtained from the supplier. The choice of coatings was made such that maximum visibility would result when used with the Si_3N_4 ball. Since the reflectivity of the Si_3N_4 ball surface was found to be 44%, one can compute the reflectivity of the coating required for visibility of 100% by equating I_1 and I_2. From Encl. 20 we have

$$I_1 = R_1 I_o = I_2 = R_2 \left[1-(R_1+A_1)\right]^2 I_o \qquad (1)$$

where I_o = intensity of incident beam

A_1 = absorption coefficient of the coating

R_1 = reflectivity of the coating

and R_2 = reflectivity of the ball surface = 0.44

Since the absorption coefficient of CeO is small it can be neglected. Therefore for CeO

$$R_1 = 0.4(1-R_1)^2 \text{ from which}$$

$$R_1 = 22.5\%$$

Due to experimental limitations, it was not possible to get a coating with R = 22.5% exactly. The cerium oxide coatings obtained all had R values between 20 and 25%. These values are considered close enough to the computed value.

In addition, silicon monoxide coatings were found to be available which offered high calculated visibility values. A few glass flats coated with SiO were ordered for trial. Their wear characteristics were found to be equivalent to those of CeO. Encl. 22 gives the computed values of the fringe visibilities for various combinations of ball and coating materials.

Encl. 23 is a comparison of static black and white fringegrams of the contact at 5 lb load, taken with glass flats coated with the three different coatings indicated in Encl. 21. The fringegrams (b) and (c) of Encl. 23 produced from the silicon cerium oxide combination, and from the silicon nitride-silicon monoxide combination, show sharp fringes for both combinations and confirm the results of the calculated visibility.

Encl. 24 also shows the very satisfactory fringes obtained in a dynamic silicon nitride-glass contact at a rolling speed of 40 in/sec and a maximum pressure of 113 ksi with a silicon monoxide coating.

On the basis of the results above, both the CeO and SiO coatings on the glass flat produce satisfactoryfringes in tests with Si_3N_4 balls.

4.2.6 Plateau Film Thickness Measurement

Due to the relative uniformity of the plateau film thickness, the contact when viewed through the eyepiece of the optical system exhibits a dominant color which corresponds to a certain film thickness. The correlation between film thickness and color can be obtained by means of a calibration process explained in Section 4.2.4 of this report. The fringe order of the color can be readily identified by increasing the speed gradually from zero.

Film thickness measurements have been completed for Mobil Jet II (Lubricant No. 1 in Enclosure 8) at a multitude of rolling speeds and two loads (5 lbs. and 15 lbs.). For comparison, both a silicon-nitride ball and steel ball were run.

The elastic modulus of Si_3N_4 is 45×10^6 psi against 30×10^6 psi for steel. The maximum Hertzian stresses under 5 and 15 lb.. loads are respectively 113 and 161 ksi for the Si_3N_4 contacts and 100 ksi and 144 ksi for the steel contacts.

In Enclosure 25 the measured plateau film thickness is plotted as a function of rolling speed at two loads for the two material combinations.

The curves show that the Si_3N_4 contact EHD film thickness is less than the steel contact at the same load by about 15-20%.

Enclosure 26 shows the measured film thickness h_o, given in Enclosure 25 divided by the theoretical unstarved film thickness h_{of} as a function of rolling speed V, where h_{of} was empirically deduced from optically measured data given in (17) for ester oils as follows:

$$h_{of} = 0.87 R \left(\frac{\eta V \alpha}{R}\right)^{0.70} \left(\frac{Q}{E' R^2}\right)^{-0.08} \qquad (2)$$

where Q = load (lbs)

η = absolute viscosity (lb-sec/in^2)

α = pressure viscosity coefficient (in^2/lb)

R = radius of ball (in)

E' = reduced Young's modulus (lb/in^2)

Enclosure 26 shows that the prediction formula fits both data sets at low velocities. As V increases h_o/h_{of} decreases indicating that the formula of Eq. (2) overestimates the film thickness at high velocity. This behavior is typical of lubricant film starvation wherein the amount of oil present in the inlet is insufficient to maintain the theoretical plateau film thickness. This explanation is confirmed by measurements made from fringegrams of the contacts of the meniscus location i.e. the distance from the contact center to the oil/air interface in the inlet region. The appearance of the curves in Enclosure 26 suggests that starvation begins at somewhat lower speeds for Si_3N_4 contacts.

The coincidence of the curves for 5 and 15 lbs. loads on this plot suggests that Eq. (2) is quite adequate in explaining the effect of load on film thickness for Si_3N_4 as well as for steel.

4.2.7 Fringegrams of Glass-Si_3N_4 Contacts

Using the ester (No. 1) oil at 5 and 15 lbs. loads, a series of fringegrams have been taken using Ansco-500 high speed color film at speeds of 5, 10, 20, 40, 60, 100, 200, 300, and 400 in/sec.

Enclosure 27 shows a selected subset of the fringegrams of the glass/Si_3N_4 contacts at two loads and three speeds. The pictures show that the meniscus location in the contact inlet moves progressively closer to the contact as speed increases. Comparison of the original color fringegrams at two loads taken at 100 in/sec (pictures C and E) show that the plateau color is the same, indicative of the low dependence of (plateau) film thickness on load. (A common color does not imply an identical film thickness since refractive index varies with pressure). An interesting feature in pictures B and C is the symmetry and sharp leading edge of the meniscus line. Meniscus lines observed with steel contacts are relatively more rounded.

The distance from the contact center to the meniscus (r^*) measured from the fringegrams and scaled by the Hertz contact radius a is plotted as the lower curve in Enclosure 28 for the Si_3N_4 contacts. The upper curve is a plot of the measured r^*/a values for the same oil measured in a previous contract (15) for steel contacts. It is seen that the steel-glass contact is somewhat less starved than the Si_3N_4-glass contact, with the difference being small at low rolling speed. The greater evident starvation for the Si_3N_4 contact can partially account for lower observed film thichnesses in Si_3N_4 contact.

A previous investigation of starvation (17) indicates that insufficient replenishment of oil between successive contacts is a cause of starvation.

In the film replenishment model, the relevant parameters are p_o/E' and a/h_∞ where p_o is the maximum pressure, a is the contact radius and h_∞ is the ambient layer height. Under a given load, both p_o and a depend on the reduced Young's modulus E'. So there is possibly some effect of E' on film replenishment rate. It is also known that increasing h_∞ corresponds to an increase in the replenishment rate. The quantity h_∞ can be dependent on the wetting characteristics of the solid surface.

In spite of the experimental evidence that the Si_3N_4 contact exhibits a somewhat earlier occurrence (i.e. at lower speed) of starvation than the glass-steel contact, the optical film thickness measurements show that a lubricated Si_3N_4 contact has satisfactory film building behavior close to what is expected by current EHD theory.

4.2.8 Traction Tests

As described in (8, 15) the traction force at the test contact in the EHD test rig is obtained from the torque measured at the ball or roller driving quill and the lateral force in the beam spring which constrains the ball or roller.

The test contact is the circular contact between the flat and the ball each of which is connected to a driving spindle. The sliding rate is defined as the difference in surface speed of the two bodies.

The following traction tests were run:

1. Typical plots of traction coefficient (defined as the sliding traction divided by normal load) against sliding speed are shown in Enclosure 29 for oil No. 6 at two loads and two rolling speeds. A glass flat and silicon nitride balls were used. It is seen that the traction rises with sliding rate and then levels off as in many previous tests conducted with steel contacts. This shape is typical for all oils except Nos. 3 and 5 which reached a maximum and then decreased with sliding speed.

2. A series of traction tests were run at three loads i.e. 5, 10 and 15 lbs. corresponding to 131, and 146 and 161 ksi maximum Hertz stress respectively. The entrainment speeds used were 40, 100 and 400 in/sec. A glass flat and silicon nitride balls were used. In Enclosure 30 the maximum traction coefficients are tabulated for the

6 lubricants at three rolling speeds and three loads. The data show that traction coefficient increases with load but decreases with rolling speed, a trend which is consistent with previous traction tests in steel contacts. The data also shows that the effect on traction of additives in paraffinic and ester oils is small as characterized by the relatively small difference in traction between oils (2) and (4) and between (1) and (6). It is found that the two ester oils (1) and (6) have higher traction than the two paraffinic oils (2) and (4). The DTE mineral oil (3) and polyphenyl ether (5) exhibit relatively high traction. The two paraffinic oils (2) and (4) have the lowest traction coefficients.

3. Enclosure 31 shows traction force data for steel/silicon nitride and steel/steel contacts. Lubricant No. 1 (Ester oil with additive) was used. These tests were run in order to assess the differences in traction coefficients in real bearings, where the contacts are silicon nitride/steel or steel/steel. In order to obtain these data a steel washer with 5 μ in surface roughness was used instead of the glass flat used in the previous investigations. It is seen from Enclosure 32 that at the highest stress level, 271 ksi, the traction force for steel/steel and steel/silicon nitride differ by no more than 8%. At the lower stress levels, 216 ksi and 247 ksi, the differences between steel/steel and steel/silicon nitride are generally larger in one case by more than 20%.

4. Enclosure 32 is a plot of the measured maximum traction coefficient at a rolling speed of 40 in/sec with an ester oil (lubricant No. 1) as a function of maximum contact pressure for three values of the axis ratio of the contact and for five material combinations. The axis ratio is 1:1 for a ball against flat contact, and differs from 1:1 for a roller against flat contact. The data points show that the traction coefficient in the silicon nitride contact is comparable or lower than that prevailing in steel contact.

4.3 Flat Washer Surface Interaction Studies

4.3.1 Description of Flat Washer Test Rig

A "Flat Washer" test rig provides a rapid and inexpensive means of obtaining fatigue data with the use of relatively simple test equipment and simple shaped specimens. The effects of parameters such as surface topography, wettability, wear resistance, and ability to generate EHD films on endurance in rolling/sliding contact may be studied with this tester.

In the SKF "Flat Washer" test rig shown in Enclosure 33, three rollers, guided by a plastic or metal cage, roll under load in a circular path between two flat washers, as shown in detail in Enclosure 34. The upper washer is stationary and the lower one rotates. The rollers are of vacuum melted M50 tool steel, hardened to Rockwell C61-64. They are 5 mm in diameter and 6 mm long, and are crowned as shown in Enclosure 35. The rollers are guided by the cage in the "aligned" position, such that the axis of the rollers intersects the common axis of the two washers. Some sliding occurs between the rollers and washers due to the curvature of the rolling path on the washers. The greatest amount of sliding occurs near the ends of the rollers, at which points the slide-to-roll ratio, may be nearly 10% with the specimen dimensions used in this test rig, and there is one point usually near the middle of each roller-to-washer contact line at which almost pure rolling (zero sliding) occurs. Lubricant is supplied to the roller/flat washer assembly at a rate of approximately 1 pint/min. from an overhead reservoir through a hollow shaft on which the upper washer is mounted. Prior to each test, the oil is filtered through a 5 μm Millipor filter. The bulk temperature of the upper washer is monitored during the tests with a thermocouple. The output of this thermocouple is monitored continuously either on a chart recorder or by a digital computer test monitoring system.

The design of the flat washer specimens of silicon nitride tested in the lower position in the flat washer tester is shown in Enclosure 36. A photograph of several flat washer testers is shown in Enclosure 37.

4.3.2 Flat Washer Test Results with Steel Specimens Only

Half-inch diameter steel balls are sometimes used in place of the rollers in the flat washer tester, as shown in the left-hand side of Enclosure 33. Endurance tests with AISI 52100 steel flat washers of different hardnesses and Hofors AOH 52100 steel balls conducted previously at SKF show that the L_{10} life deviates most drastically from predicted behavior in a critical stress range depending on hardness (life drops by a factor of 5 to 10 below that extrapolated from either higher or lower stress data), the lower hardness washers having a reduced life region in a lower load range. Rockwell 63C and 61C hardness washers were tested, as shown in Enclosure 38, on which each point represents about thirty flat washer fatigue tests. Similar results were obtained with Rockwell 64.5C balls rolling together in a rolling 4-ball tester, also shown plotted in Enclosure 38.

Indications are that the life of rolling contacts is decreased below expected values in critical contact stress ranges where the onset of gross plastic deformation is allowed to take place probably resulting in sub-surface residual stresses formed in such a manner that the amplitude of the maximum sub-surface reversing orthogonal shear stress is increased. (This stress is considered the critical stress in rolling fatigue failure.)

It was observed that considerable plastic grooving occurred in the ball track of the flat washers tested with balls and that the groove radius increased with decreasing load. In order to minimize this variable of grooving on life, testing has been conducted on a flat washer against cylindrical roller configuration as shown in Enclosure 34. The L_{10} life obtained from tests conducted previously at SKF on 52100 steel flat washers of 61 Rc in the roller-flat washer configuration exceeds the theoretical life calculated by the 4th power method (24) in contrast with results obtained in ball-flat washer tests. This is shown graphically in Enclosure 39 where a comparison is given between the theoretical load-life behavior and the experimental load-life for both the L_{10} (10%) life and the L_{50} (50%) life. The deviation from a linear relationship produced at the lower load can be related to the use of rollers with excessive crown.

Endurance data on the rollers in a flat washer/roller configuration has been collected previously at SKF on manufacturing lot of 5 x 6 mm "triple crowned" (crown drop of 2-2.5 µm at the measuring point on one side equal to ~3.3 times the Lundberg crown drop for 1200 lbs. washer load) rollers made from consumable electrode vacuum melted (CVM) M-50 tool steel. Flat washer testers (Enclosure 37) with circulating Mobil DTE medium heavy lubricant were used.

Test conditions were 3400 rpm, 250°F, and three load values. Summarized in the table below are the detailed life data obtained:

Group	Test Load	Max. Hertz Stress, KSI	Theoretical Life Of Assembly L10 Mill. Revs.	Theoretical Life* of Roller Set L10 Mill. Revs.	Number of Tested Roller Sets	Number of Failed Roller Sets	Max. Likelihood* Estimated L10 Mill. Revs.
3141, 3142	1200#	315	1.15	2.8	45	9	8.4
3143, 1751, 1755	1000#	280	2.44	4.76	62	8	18.3
3144	800#	255	5.9	12.4	30	1	**

The experimental lives of CVM M-50 rollers run against steel flat-washers are in excess of 3-1/2 times the theoretical 4th power roller set life. These lives are not significantly different from the 5 times calculated life often quoted for CVM M-50 rings. If one considers the severe operating conditions in a flat washer test (spin, low speed, low C/P) the results support the life prediction of 4 to 5 times calculated life for CVM M-50 steel under application conditions.

4.3.3 Test Results with Silicon Nitride Washers

Enclosure 40 shows endurance test results on seven flat washer assemblies run on the present program. The top washer was made of 52100 steel in all tests. The bottom washer was made of 52100 steel in two of the tests and of silicon nitride having as-ground surface finish (5 microinches, AA) in the remaining five. The rollers were made of CVM M-50 tool steel in five tests and Rex 49 tool steel in two tests. The speed was 3330 rpm and the load 1000 lbs. except for one test where the load was 500 lbs. The lubricant was MIL-L-23699. It is seen that every failure was due to spalled or distressed rollers. Enclosure 41 is a Weibull plot of the test data in Enclosure 40, excluding Test 3, because of the lower load in this test. The Weibull slope of the data in Enclosure 41 is 1.36. This value is within the range usually obtained in bearing endurance testing and indicates that the life variations are not necessarily due to differences in flat and roller materials, but rather to expected random variations within the sample of six washer assemblies.

---

* Life estimates calculated and bias corrected per (25).
**Life in excess of 80 M.R.

The estimated L_{10} life of this group shown in Enclosure 41 is about 0.2 million revolutions, or about a factor of 100 below the estimated L_{10} of 18.3 million revolutions for 62 roller sets tested previously in these testers with DTE medium heavy mineral oil lubrication, as shown in the above tabulation. It was noted in the recent tests that the roller and steel washer track surfaces, where steel washers were used, suffered lubrication distress. The silicon nitride flats had a groove about 20 microinches deep worn in their tracks and the rollers against which they ran were especially distressed. Subsequent testing of steel washers in this rig with DTE medium heavy mineral oil lubrication has produced significantly longer lives, thus indicating that the low endurance lives of Tests No. 1 and 2 in Enclosure 40 with steel washers were the result of a life reduction due to excessive lubrication distress with the MIL-L-23699 lubricant in this tester operating under the severe conditions of high sliding, low speed and high load. Apparently under these severe conditions significant wear of the silicon nitride occurs, causing very early spalling failure of the tool steel surface of the rollers against which it is run. Since these contact conditions are typical of the high-spinning high-load critical inner-ring contacts of ultra-high-speed turbine-engine mainshaft angular-contact ball bearings, further studies of these phenomena is needed and is currently in progress.

4.4 Sliding Friction and Wear Studies

4.4.1 Characterization of Surface Finish

The random microgeometry of surfaces in rolling contact has been recognized in recent years as a major determinant of the contact's fatigue, wear and traction behavior. Measurements of the center line average (CLA) or root mean square (RMS) height of a profile trace are standard methods to characterize the degree of roughness of the surfaces. The ratio h/σ of EHD film thickness h to the composite RMS surface roughness height σ, with $\sigma^2 = \sigma_1^2 + \sigma_2^2$ and σ_1, σ_2 the RMS roughness amplitudes of two mating lubricated surfaces, has become a widely accepted measure of the efficacy of the lubrication conditions in rolling contact.

In unlubricated conditions or when less than full film exists ($h/\sigma < 3.0$), asperities interact and the degree of plastic working that results has been observed to depend on the slopes of the asperities and not just upon the CLA or RMS height.

Accordingly, the SKF Research Laboratory developed a device which operates in conjunction with a Talysurf instrument to yield RMS values of the profile slope in the direction of tracing.

A problem in the characterization of surfaces by means of one-dimensional profile data is the fact that a biased impression is thereby obtained of the summit heights and slopes on the two-dimensional surface. Both are understated in profiles. This is particularly true of surfaces having strong directionality such as the one shown in Enclosure 42. Since the sliding friction coefficient, and hence the wear rate, are different for motion along and across the furrows it becomes necessary to characterize the surface finish more completely.

Recent theoretical developments permit the deduction of two-dimensional surface characteristics from profile measurements of RMS height and RMS slope, the latter being taken in at least three known directions. It is possible, using such a group of RMS slope measurements, to characterize the degree of anisotropy of the surface by finding the pair of orthogonal directions along which the RMS profile slope is maximum and minimum and the value of these extreme RMS slopes.

4.4.2 Theory of Longuet-Higgins on Surface Microgeometry Characterization

A surface whose statistical description is independent of the direction of (profile) measurement is called an isotropic surface. Due to the directionality of processing operations, most real surfaces have statistics that depend on the direction of profile measurement. Surfaces that have direction-dependent statistical descriptions are called anisotropic.

Williamson (19) has shown that a large variety of surfaces encountered in engineering practice are Gaussian, i.e. the distribution of surface heights follows a Gaussian or normal distribution. A Gaussian assumption will be made here.

Surface statistics are most usually deduced from analyzing profile traces made by a displacement sensitive stylus traversing the surface. This is the principle of operation of the Talysurf instrument widely used for this purpose. The assumption is made that the tip radius of the stylus is small compared to the features to be traced.

One-dimensional profile traces yield distorted information regarding the actual two-dimensional roughness process, but until Nayak (20) unearthed the little-known work of Longuet-Higgins (21), there was no commonly known method for compensating for this distortion.

Longuet-Higgins derived the relationship between the one-dimensional spectral moments of a profile and the two-dimensional spectral moments of a surface.

A description of a portion of the Longuet-Higgins paper applicable to this study is given in Appendix I.

The profile statistics method by Longuet-Higgins was applied to a flat silicon nitride specimen. The necessary measurements were obtained on a Talysurf instrument (model No. 4). The value of $\sigma^2 = m_{00}$ was obtained directly on a CLA meter. Values of m_{00} and m_{20} were obtained at 11 different angles of measurement equally spaced at 15° intervals as shown in Enclosure 43.

A computer program for linear regression analysis was used to compute least squares estimates of the quantities m_{20}, m_{11} and m_{02} using the measured value of $m_{2\theta}$ as the dependent variable and $x_1 = \cos^2\theta$, $x_2 = \sin 2\theta$ and $x_3 = \sin^2\theta$ as independent variables according to Eq. (4) of Appendix I.

The result was found to be

$$m_{2\theta} = 9.15 \cos^2\theta - 0.0759 \sin 2\theta + 18.56 \sin^2\theta$$

The principal direction is calculated in Eq. (5) of Appendix I to be

$$\bar{\theta} = 90^\circ 27'$$

i.e. consistent with the obvious directionality seen in Enclosure 42.

From the above equation one has,

$$(m_2)_{max} = 18.56$$

$$(m_2)_{min} = 9.15$$

Thus the RMS slope angle varies with tracing direction between a maximum of 4.3° and a minimum of 3.0°, a rather modest degree of anisotropy.

4.4.3 Experimental Study of Friction and Wear Using "Pin on Disk" Apparatus and Lapmaster.

Attached in their entirety as Appendix II are Professor Rabinowicz's four quarterly reports on friction and wear tests conducted at MIT with hot pressed silicon nitride and other ceramic specimens. In the friction tests a simple "pin on disk" apparatus was used. The top specimen, a 1/4" rod was pressed against the bottom specimen, a plate rotated at a speed of 0.3 cm/sec in the friction tests and 30 cm/sec in wear tests. Wear tests were conducted in a "Lapmaster" machine. Enclosure 44 shows a scanning electron micrograph (SEM) taken at SKF of the wear debris produced in a typical

Lapmaster test with silicon nitride. This photograph shows the presence of faceted particles typical of brittle fracture. The most important findings in this study, including the SEM work at SKF, are:

1. The results indicate that the friction coefficient on ground silicon nitride surfaces seems to be lower when the pin traverses across the grinding grooves than when it runs parallel to the grooves.

2. Some of the six lubricants tested give a higher friction coefficient than the unlubricated condition. The silicone gives a much higher friction coefficient than all the other lubricants. The hydrocarbon Teresso V78 gave the lowest friction coefficient, by a slight margin. Turbojet 2380 oil was later added to the list and found to have almost the same friction coefficient as Teresso V78.

3. These studies suggest that silicon nitride behaves in a brittle fashion on a microscale at least under surface finishing conditions.

LIST OF REFERENCES

1. Rumbarger, J. H. Dunfee, J. D. "Survey of the State of the Art For the Design of High Speed Rolling Element Bearings in Gas Turbine Engines", Franklin Institute Research Lab., Report F-C2138-1 under Contract N00156-68-C-0330.

2. Leonard, L., Cotellesse, G., and Erhardt, K., "Final Report on Scanning Electron Microscopy Study of 6309 Size Bearings", U.S. Department of the Navy, Office of Naval Research, Contract N00014-70-C-0229, SKF Report AL71C002 (1971).

3. Three papers on Rolling Bearing Mathematical Failure Models: (1) "An Engineering Model of Spalling Fatigue in Rolling Contact - Engineering Discussion and Illustrative Examples", by T. E. Tallian, (2) "An Engineering Model of Spalling Failure in Rolling Contact - The Surface Model", by T. E. Tallian, J. I. McCool and (3) "An Engineering Model of Spalling Fatigue Failure in Rolling Contact - The Subsurface Model", by Y. P. Chiu, T. E. Tallian, J. I. McCool. Published in Wear, 17, 433-480 (1971).

4. Sibley, L. B., et al, "A Study of Refractory Materials for Seal and Bearing Applications in Aircraft Accessory Units and Rocket Motors", WADC Technical Report 58-299 (1958).

5. Sibley, L. B. et al, "Characteristics Governing the Friction and Wear Behavior of Refractory Materials for High Temperature Seals and Bearings", WADD Technical Report 60-54 (1960).

6. Taylor, K. M. Sibley, L. B., Lawrence, J. C., "Development of a Ceramic Rolling Contact Bearing for High Temperature Use", Wear, 6, 266-40 (1963).

7. Parker, R. J. and Zaretsky, E. V.: "Rolling-Element Fatigue Life of Silicon Nitride Balls-Preliminary Test Results", NASA Technical Memorandum NASA TMX-68174, Nov. 1972.

8. J. I. McCool, H. Dalal and W. E. Jamison, "Surface Interactions and Lubrication Response of Silicon Nitride Bearing Elements", First Quarterly Report, U.S. Department of the Navy, Contract N00019-73-C-0150, SKF Report AL73P005 (March, 1973).

LIST OF REFERENCES (CONTINUED)

9. J. I. McCool, H. Dalal and Y. P. Chiu, "Surface Interactions and Lubrication Response of Silicon Nitride Bearing Elements", Second Quarterly Report, U.S. Department of the Navy, Contract N00019-73-C-0150, SKF Report AL73P017 (June 1973).

10. H. Dalal, Y.P. Chiu and J. I. McCool, "Surface Interactions and Lubrication Response of Silicon Nitride Bearing Elements", Third Quarterly Report, U.S. Department of the Navy, Contract N00019-73-C-0150. SKF Report AL73P026 (December 1973).

11. N. K. Adam and G. Jessop, J. Chem. Soc., 1863 (1925).

12. Private communication, G. Bersch, NASc (1972).

13. McLean, A. F., Fisher, E. A. and Bratton, R. J. "Brittle Materials Design, High Temperature Gas Turbine", ARPA Contract No. DAAG46-71-C-0162.

14. Lange, F. F., "Fabrication and Properties of Silicon Compounds," Westinghouse Research Laboratories, Final Report, Naval Air Systems Command, Department of the Navy, Contract No. N00019-72-C-0278.

15. Y. P. Chiu et al., "Exploratory Analysis of Elastohydrodynamic Properties of Lubricants", Final Summary Report, U.S. Navy Contract No. N00019-71-C-0425.

16. Wedeven, L. D., Evan D. and Cameron, A., "Optical Analysis of Ball Bearing Starvation", J. Lub. Tech., Vol. 93, No. 3, pp. 349-261, (July, 1971).

17. Y. P. Chiu, "An Analysis and Prediction of Lubricant Film Starvation in Rolling Contact Systems", ASLE Transactions, Vol. 17, No. 1, p. 22, 1974.

18. C. A. Foord et. al., "Optical Elastohydrodynamics", Inst. of Mech. Engrs., February 1970.

19. J. B. P. Williamson, "The Shape of Solid Surfaces", Surface Mechanics, Proceedings of the ASME Winter Meeting, Los Angeles, California, 16-20, November, 1969.

20. P. R. Nayak, "Random Process Model of Rough Surfaces", J. of Lub. Tech., Vol. 93, No. 3, p. 398, 1971.

LIST OF REFERENCES (CONTINUED)

21. Longuet-Higgins, M.S., "Statistical Properties of Anisotropic Random Surface", Philosphical Trans. of the Royal Society Vol. 250, Series A, p. 157, 1957.

22. Gielisse, P. J., "Ceramic Materials for High Temperature Gas Bearings", ONR Annual Report on Contract No. N00014-68-A-0215-008, Univ. of Rhode Island, Report AD 753858 (September, 1972).

23. Wheildon, W. M.; Baumgartner, H. R.; Sundberg, D. V.; and Tort, M. L., "Ceramic Materials in Rolling Contact Bearing," Final Report, Naval Air Systems Command, Department of the Navy, Contract No. N00019-72-C-0299.

24. Lundberg, G. and Palmgren, A., Dynamic Capacity of Rolling Bearings, Acta Polytechnica No. 196 (1947); see also Dynamic Capacity of Roller Bearings, Acta Polytechnica No. 210 (1952).

25. McCool, J. I., "Evaluating Weibull Endurance Data by the Method of Maximum Likelihood", ASLE Transactions 13, 189-202, (1970).

APPENDIX I

A DESCRIPTION OF A PORTION APPLICABLE TO THE PRESENT STUDY OF THE PAPER "STATISTICAL PROPERTIES OF ANISOTROPIC RANDOM SURFACE" BY M. S. LONGUET-HIGGINS

The definition of spectral moments is as follows: If the power spectrum of the two-dimensional height process is $\pi(\omega_x \omega_y)$ and that of a profile traced in the direction θ relative to x is $\pi_\theta(\omega)$, then the two-dimensional spectral moment of order p, q is

$$m_{pq} = \iint_{-\infty}^{+\infty} \pi(\omega_x \omega_y)\, \omega_x^p \omega_y^q \, d\omega_x \, d\omega_y$$

and the profile spectral moment of order n is $m_{n\theta} = \int_{-\infty}^{+\infty} \pi_\theta(\omega)\omega^n d\omega$

The first two non-zero spectral moments of a profile are designated m_0 and m_2. (In a symmetrical (Gaussian) process, odd order moments vanish). m_0 is identical to the variance σ^2 of the roughness amplitude process, and m_2 is the variance of the slope of the roughness process in the θ direction.

Of the two-dimensional spectral moments of the surface (with two subscripts), the lowest order non-zero values are m_{00}, m_{20} and m_{02}.

If a cartesian coordinate system is arbitrarily established on a rough surface and a profile trace is made at an angle θ to the x axis of this coordinate system, the profile moments $m_{0\theta}$ and $m_{2\theta}$ are, according to Longuet-Higgins, related to the two-dimensional spectral moments as follows:

$$m_{0\theta} = m_{00} = \sigma^2 \qquad (3)$$

$$m_{2\theta} = m_{20}\cos^2\theta + 2m_{11}\sin\theta\cos\theta + m_{02}\sin^2\theta \qquad (4)$$

Eq. (3) shows that the RMS roughness height is independent of θ.

Eq. (4) shows that m_{20} is equal to m_2 for a profile in the direction $\theta = 0$, i.e. a profile taken along the x axis. Similarly, m_{02} is the value of m_2 from a profile trace along $\theta = \pi/2$. Since m_2 is a variance, it cannot be negative in any direction, and hence it follows that m_{02} and m_{20} are positive quantities.

For an isotropic surface $m_{2\theta}$ is by definition independent of θ and hence for an isotropic surface one must have, regardless of the orientation of the coordinates:

$$m_{11} = 0$$

$$m_{20} = m_{02} = m_2$$

If <u>either</u> m_{11} differs from zero, <u>or</u> m_{20} and m_{02} from each other, then the surface is anisotropic.

For given values of m_{20}, m_{02} and m_{11} Eq. (4) above yields the profile slope variance $m_{2\theta}$ as a function of θ, i.e. it represents $m_{2\theta}$ in a polar coordinate system with coordinate angle θ.

It can be shown that another polar system can always be obtained by an axis rotation through the angle $\bar{\theta}$, in which the term m_{11} vanishes. The required angle of rotation is given by

$$\bar{\theta} = \frac{1}{2}\tan^{-1}\left(\frac{2m_{11}}{m_{20} - m_{02}}\right) \tag{5}$$

The form of the equation in the new system is

$$m_{2\theta} = \bar{m}_{20}\cos^2\phi + \bar{m}_{02}\sin^2\phi \tag{6}$$

where

$$\phi = \theta - \bar{\theta} \tag{7}$$

$$\bar{m}_{20} = m_{20}\cos^2\bar{\theta} + m_{11}\sin 2\bar{\theta} + m_{02}\sin^2\bar{\theta} \tag{8}$$

and

$$\bar{m}_{02} = m_{20}\sin^2\bar{\theta} - m_{11}\sin 2\bar{\theta} + m_{02}\cos^2\bar{\theta} \tag{9}$$

Note that $\bar{m}_{20}+\bar{m}_{02}= m_{20}+m_{02}$ irrespective of $\bar{\theta}$, i.e. the sum of the coefficients of the $\sin^2$ and $\cos^2$ terms is invariant with respect to an axis rotation.

The maximum value of m_2 is readily shown to occur at $\phi = 0$ and the minimum at $\phi = \pi/2$, thus

$$(m_2)_{max} = \bar{m}_{20}$$

and

$$(m_2)_{min} = \bar{m}_{02}$$

The directions $\bar{\theta}$ and $\bar{\theta}+\pi/2$ with respect to the original axis are the principal directions for m_2 , i.e. m_2 is maximum in the direction $\bar{\theta}$ and minimum in the direction perpendicular to $\bar{\theta}$.

AL74P009

APPENDIX II

FRICTION AND WEAR TESTS WITH HP SILICON NITRIDE

by

Professor Ernest Rabinowicz
Massachusetts Institute of Technology

APPENDIX II

FIRST QUARTERLY REPORT

Introduction

The starting material for these tests were a silicon nitride rod of length 1" and diameter 1/4", with a trunkated conical end, also a silicon nitride plate of dimensions 2" x 2" x 1/4". These were kindly supplied to me on a no-charge basis by Norton. Tests have been carried out using these materials as well as similarly shaped specimens of M 50 steel.

As received, the silicon nitride flat had a ground finish with surface roughness approximately 24 microinches RMS. In carrying out friction tests using a rider sliding circumferentially on the disk, there was a sharp rise in friction whenever the rider moved parallel to the grinding grooves. In later tests, the surface finish was improved to about 4 microinches RMS by lapping the flat on a Lapmaster with 600-grit abrasive. Friction and wear results have also been obtained on this smoother surface.

It was noticed that the rate of removal of silicon nitride on the Lapmaster was excessively high. Tests on other ceramic materials have been conducted to check out this impression, and these tests are also described below.

Apparatus

The simple pin on disk apparatus used in the friction and wear tests is shown in Figure 1. The top specimen, the 1/4" rod, was pressed against the bottom specimen under a load which was generally 2 kg. The bottom specimen, the plate, was rotated at a speed of

0.3 cm/sec in the friction tests and a higher speed of 30 cm/sec in the wear tests. In order to obtain measurable amounts of wear, the wear tests generally lasted many hours. For lubricated tests, the bottom plate was covered by the lubricant in question.

Results

A. Friction coefficient f

	Si_3N_4 on Si_3N_4 (ground) along groove	Si_3N_4 on Si_3N_4 (ground) across groove	Si_3N_4 on M50	M50 on Si_3N_4 (ground) along groove	M50 on Si_3N_4 (ground) across groove	M50 on Si_3N_4 (lapped)
Unlubricated	.17	.17	.16	.16	.15	.16
Cetane	.20	.15		.16	.12	
Palmitic acid in cetane	.17	.15		.17	.11	
Silicone DC 200-50	.24	.24		.36	.36	.36
Fluorocarbon Halocarbon 11-14	.17	.15	.16	.17	.16	.16
Ucon fluid DLB 180 BX	.17	.15	.17	.15	.12	.13
Hydrocarbon Teresso V78	.16	.13	.13	.16	.11	.14

It will be seen that combination involving rough surfaces (i.e. Si_3N_4 flats, sliding along the groove) generally gave friction coefficients of about .16-.17, more or less the same as for unlubricated surfaces. In contrast, smooth Si_3N_4 surfaces frequently gave friction coefficients in the range .11-.14. The silicone was a terrible lubricant, especially in combinations involving M 50 steel.

B. Wear coefficient k

This is obtained via Archard's formula

$$k = \frac{3 \times \text{penetration hardness} \times \text{wear volume}}{\text{load} \times \text{sliding distance}}$$

In this case the wear volume was always the total volume lost from both surfaces, while the hardness was that of the softer member of the pair, either M 50 at 800 kg/mm^2 or Si_3N_4 at 1500 kg/mm^2.

	Si_3N_4 on Si_3N_4 (ground)	Si_3N_4 on M50	M50 on Si_3N_4 (ground)	M50 on Si_3N_4 (lapped)
Unlubricated	5600×10^{-6}	220×10^{-6}	50×10^{-6}	20×10^{-6}
Palmitic acid in cetane		30	85	
Teresso V78				3.2

For a non-metallic sliding system (either non-metal against non-metal or non-metal against metal), we would generaly expect wear coefficients of about 5×10^{-6} unlubricated and 2×10^{-6} lubricated. E. Rabinowicz, Friction and Wear of Materails, John Wiley and Sons, New York, 1965, p. 164. Indeed, the system M 50 on lapped Si_3N_4 lubricated by Terresso V78, did give a wear coefficient in this range. The other wear values were higher, often much higher, suggesting that brittle fracture wear was occurring.

C. Wear in the Lapmaster apparatus

The wear of various ceramic materails was determined, and an abrasive wear coefficient $\overline{\tan\theta}$ was computed, according to the formula

$$\overline{\tan\theta} = \frac{3 \times \text{wear volume} \times \text{hardness}}{\text{Load} \times \text{distance slid}}$$

The values obtained were as follows

Material	Estimated Hardness	Measured $\overline{\tan\theta}$ value
GE 330 tungsten-titanium carbide	1250 kg/mm^2	3×10^{-3}
HP Si_3N_4	1500	30×10^{-3}
Silicon carbide	2000	1×10^{-3}
Boron carbide	2500	5×10^{-3}

For three-body abrasion processes, as in a Lapmaster, $\overline{\tan\theta}$ values of 2 to 6 x 10^{-3} might be considered normal. The silicon nitride falls way outside this range, suggesting again that brittle fracture has occurred.

Discussion

It is too early to make any definite statements about the friction and wear properties of Si_3N_4, but our samples appear to be brittle, and there seems to be considerable sensitivity to surface roughness.

Future tests will, hopefullv, explore these and other variables more fully. We plan to run a few tests involving other ceramic materials, to see to what extent silicon nitride is characteristic, and also to run tests involving lubricated silicon nitride at elevated temperatures.

As further samples of silicon nitride become available, perhaps manufactured in slightly different wavs, it mav be of interest to evaluate them in the Lapmaster. I have a hunch that samples which show a low wear rate under abrasive conditions will also show low wear rates under ordinary sliding conditions.

APPENDIX II (CONTINUED)

SECOND QUARTERLY REPORT

Introduction

During the past three months, the main focus of our investigations has been to generate further data on the friction of lubricated pairs of materials, one of which is silicon nitride or some other ceramic. The aim here is to see to what extent the frictional properties of silicon nitride are exceptional or anomalous.

At the same time, we have had the opportunity to carry out further wear tests of other silicon nitride samples on the Lap-master, our aim here being to see if this technique is able to measure the structural integrity of various silicon nitride samples. These results, too, are presented below.

Results

A. Friction tests

The data were obtained under the identical conditions as those described in the first quarterly report. A pin on disk tester was used, and the top specimen, a 1/4" rod, was pressed into the bottom specimen under a load of 2 kg. The bottom specimen, the plate, was rotated at a speed of 0.3 cm/sec.

The specimens used in these tests consisted of a tungsten-titanium carbide (GE 330), silicon carbide (Crystallon N), boron carbide, as well as the Norton-derived hot pressed silicon nitride specimens used in previous tests.

Table I. Friction Coefficient Values

	WC on WC	M50 on WC	Si_3N_4 on WC	SiC on SiC	M50 on SiC	Si_3N_4 on SiC
Unlubricated	.34	.19	.22	.52	.29	.31
Silicone DC 200-50	.40	.39	.33	.23	.42	.35
Fluorocarbon Halocarbon 11-14	.20	.18	.18	.14	.14	.14
Ucon Fluid DLB 180 BX	.21	.16	.14	.20	.16	.17
Hydrocarbon Teresso V78	.18	.13	.18	.14	.13	.15

	B_4C on B_4C	M50 on B_4C	Si_3N_4 on B_4C	M50 on M50
Unlubricated	.53	.29	.43	
Silicone	.28	.30	.34	
Fluorocarbon	.27	.25	.31	.15
Ucon Fluid	.23	.20	.31	.20
Hydrocarbon	.25	.25	.29	.12

B. Wear tests on the Lapmaster machine

These tests were carried out under the same conditions as those described in the last report, using a load of 1 kg, a sliding speed of 30 cm/sec, ana 600 grit silicon carbide as abrasive. The duration of the tests was 1-2 hours. The results are shown below.

Table II. Abrasive Wear Coefficient Values Obtained on the Lapmaster

Specimen	Wear Coefficient Value ($\tan \theta$)
H.P. Si_3N_4 flat, 2" x 2" x 1/4" Used in previous tests Obtained from Norton.	[illegible]0 x 10^{-3}
H.P. Si_3N_4 ring, 1 3/8" OD, 13/16" ID, 5/8" long Kindly lent by Dr. H. Mahnke, SKF Obtained from Norton.	8 x 10^{-3}
H.P. Si_3N_4 flat, 2 1/4" x 2 1/4" x 1/4" Purchased for this program from Norton.	80 x 10^{-3}

The range in wear coefficient values is quite marked. It is of interest to note that the most recently obtained specimen may indeed be the worst, in terms of structural integrity.

Discussion

Looking at the friction results, and comparing them with those presented in the last report, there seems little unusual in the frictional properties of Si_3N_4 as compared to those of other hard non-metallics. Silicon nitride gives relatively high friction with the silicone fluid, but so do the other materials. The general range of lubricated friction values is also typical. Perhaps the only unique thing about silicon nitride is the exceptionally low friction coefficient of .17 for the unlubricated material sliding on itself.

The wear values obtained on the Lapmaster show a lot of scatter. In future tests, we plan to see if these wear values correlate with other frictional properties of these samples.

APPENDIX II (CONTINUED)

THIRD QUARTERLY REPORT

Introduction

During the period covered by this report, a number of friction tests were run using a sample of the lubricant Turbojet 2380 (MIL L 23699 Exxon) obtained from SKF, to see how this practically important lubricant would perform. At the same time, adhesive wear tests were carried out using the new samples of silicon nitride recently obtained from Norton. The results of this testing are shown below.

Results

A. Friction tests using Turbojet 2380

The data was obtained under the same conditions as those described in earlier reports using a pin on disk tester in which a 0.25" diameter rod is pressed against a flat specimen. The normal force was 2 kg and the speed of rotation was 0.3 cm/sec.

The results obtained are shown in Table I. For comparison, results obtained with Teresso V 78 (a mineral oil used as a general purpose lubricant), and shown in earlier reports, are also given.

Table I. Values of the friction coefficient f

Material combination	f with Turbojet 2380	f with Teresso V78
Silicon nitride on silicon nitride	.12	.13
M 50 steel on silicon nitride	.11	.11
Boron carbide on silicon nitride	.24	.29
Boron carbide on boron carbide	.31	.25
M 50 steel on boron carbide	.24	.25
M 50 steel on M 50 steel	.13	.12

It will be seen that the Turbojet and the Teresso produced almost the same friction values each time. Also significant is the fact that both silicon nitride on silicon nitride and M 50 steel on silicon nitride are combinations which give quite low friction values. Thus, these are combinations which can be readily lubricated.

B. Wear tests using Turbojet 2380

The tests were carried out using specimen of HP silicon nitride recently obtained from Norton. The results obtained are shown in Table II. For comparison, a result reported earlier using another sample of HP silicon nitride is also shown.

Table II. Values of the wear coefficient k

Combination	k with Turbojet 2380	k with Teresso V78
Silicon nitride on silicon nitride	2.2×10^{-6}	
M 50 steel on silicon nitride	1.0×10^{-6}	3.2×10^{-6}

These k values are quite reasonable for well lubricated sliding systems involving non-metallic materials. (For such combinations, the book "Friction and Wear of Materials," E. Rabinowicz, Wiley, 1965, suggests on p. 164 a wear coefficient of 2×10^{-6}).

Future tests

Currently we have under way an exploratory series of tests to compare the abrasive wear properties of silicon nitride samples with other mechanical properties of these same samples, in an attempt to see if abrasive wear testing can form the basis of a simple materials test for selecting good samples of silicon nitride.

Following this work, we have scheduled a series of tests to measure the friction and wear of lubricated silicon nitride at elevated temperatures. It is important to see whether the good friction and wear behavior of lubricated silicon nitride at room temperature extends to elevated temperatures.

APPENDIX II (CONTINUED)

FOURTH QUARTERLY REPORT

The 3-pin high temperature friction test apparatus was repaired. Friction-temperature tests were conducted using four combinations of Si_3N_4 and M-50 riders and flats.

The test conditions and test results are listed in Table 1. Plates 1 and 2 present the same information in graphical form.

TABLE 1

TEST CONDITION	TEMP. (°C)	FRICTION COEFF.
M-50 riders on Si_3N_4 flat, lubricated with MIL-L-23699	36	0.122
	85	0.126
	150	0.128
	200	0.130
Si_3N_4 riders on Si_3N_4 flat, unlubricated Run 1	30	0.126-0.180
	105	0.122-0.173
	150	0.155-0.180
	180	0.158-0.183
	200	0.155-0.180
Same condition as above, Run 2	28	0.151-0.173
	50	0.158-0.180
	110	0.158-0.184
	150	0.169-0.187
	200	0.173-0.194
Si_3N_4 riders on M-50 flat, lubricated with MIL-L-23699	32	0.152
	90	0.157
	155	0.161
	200	0.165
Si_3N_4 riders on Si_3N_4 flat, lubricated with MIL-L-23699	33	0.126
	90	0.126
	145	0.130
	180	0.137
	200	0.144

TABLE I, cont.

TEST CONDITION	TEMP. (°C)		FRICTION COEFF.
Si_3N_4 riders on Si_3N_4 flat; lubricated with Teresso V-140 and V-65 (volume ratio 1:4.8)	29		0.104
	80		0.115
	150		0.132
	200		0.145
	250		0.156
M-50 riders on M-50 flat, lubricated with MIL-L-23699	28		0.110
	85		0.115
	160		0.123
	213		0.128
	250		0.134
Si_3N_4 riders on Si_3N_4 flat, lubricated with palmitic acid in cetane	33		0.116
	85		0.116
	150		0.116
	200		0.116
	250		0.116
Si_3N_4 riders on Si_3N_4 flat, lubricated with Halocarbon 11-14	28		0.126
	80		0.140
	150		0.160
	200		0.182
	210	(stick-slip) ↓	0.185
	230		0.193
	250		0.200

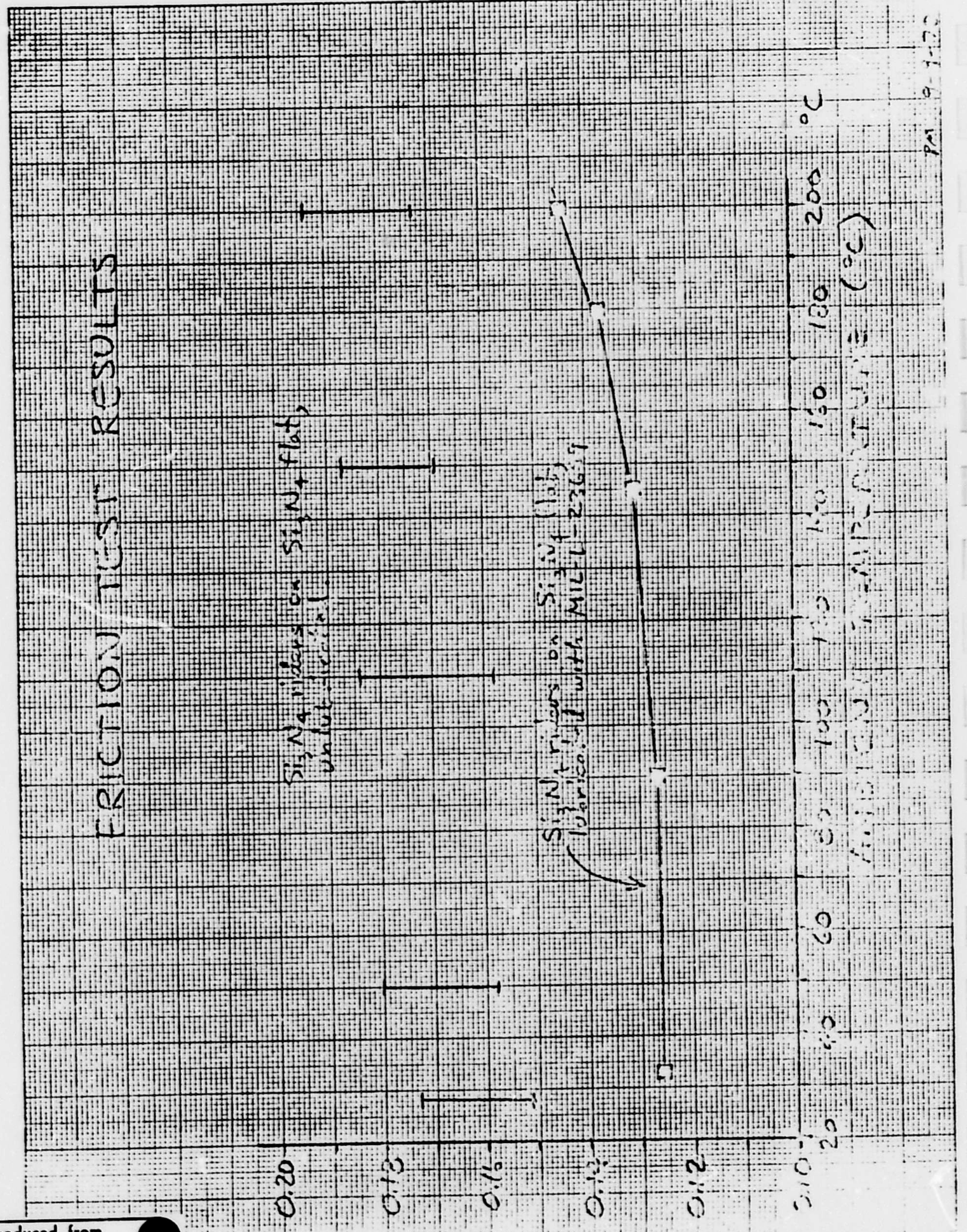
FRICTION TEST RESULTS
0.20
0.18
0.16
0.14
0.12
0.10
20
40
60
80
100
120
140
160
180
200
°C

L74P 009

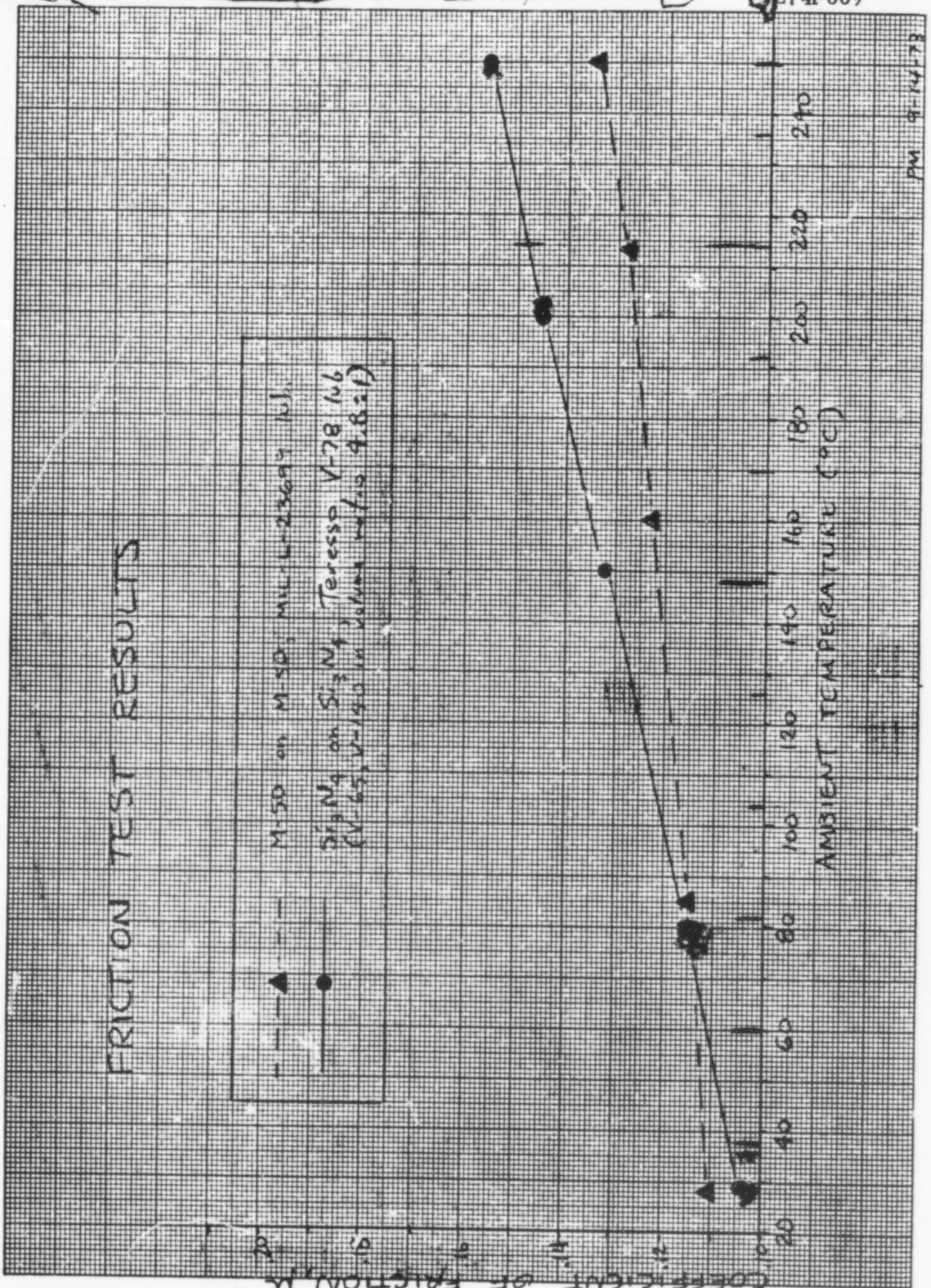

II/17-

RESEARCH LABORATORY SKF INDUSTRIES, INC.

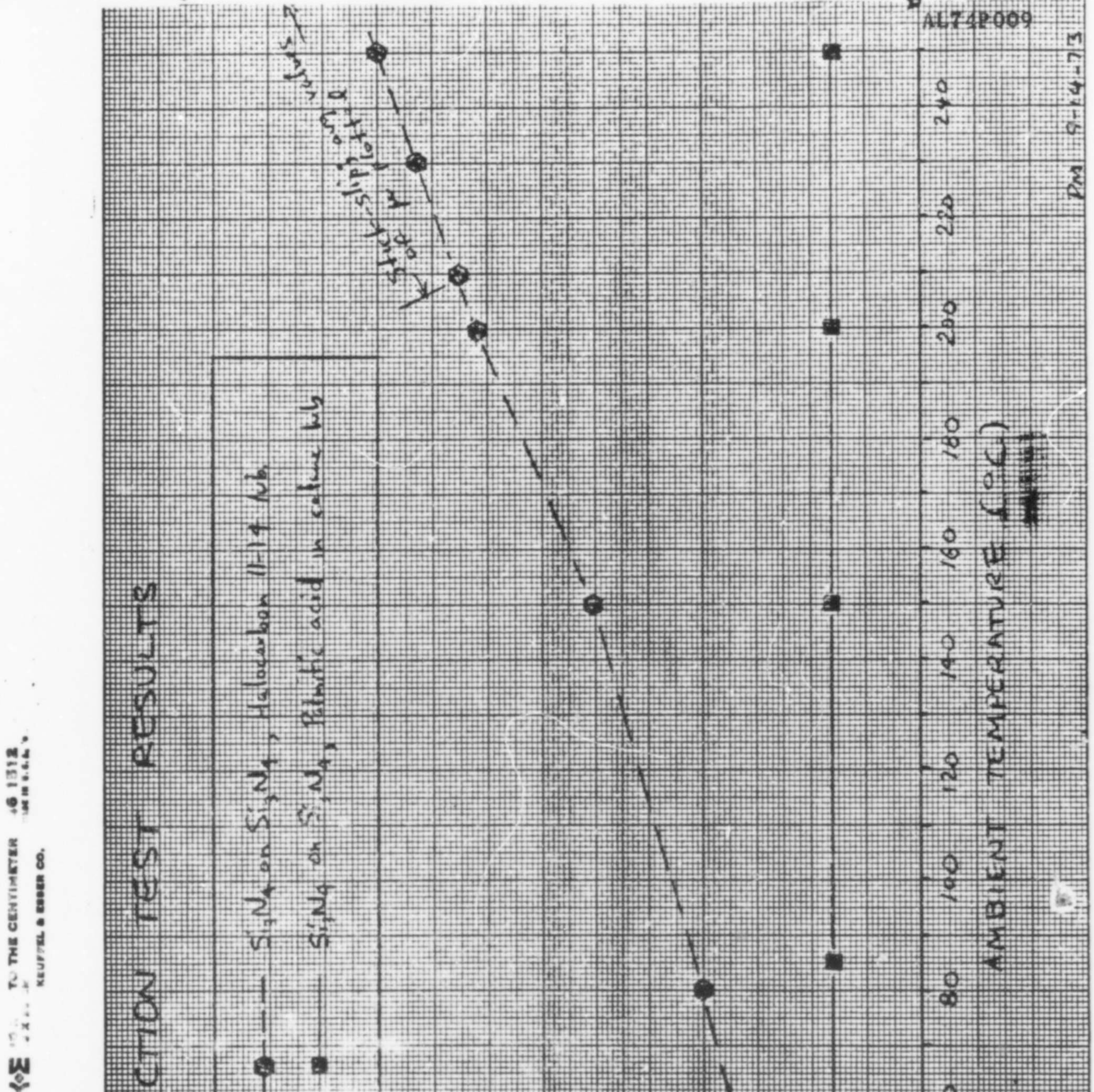

AL74P009
FRICTION TEST RESULTS
Si_3N_4 on Si_3N_4, Halocarbon 11-14 lub.
Si_3N_4 on Si_3N_4, Palmitic acid in cetane lub.
Stick-slip on all values of μ plotted
COEFFICIENT OF FRICTION, μ
.10
.12
.14
.16
.18
.20
AMBIENT TEMPERATURE (°C)
20
60
80
100
120
140
160
180
200
220
240
PM 9-14-73
KEUFFEL & ESSER CO.
TO THE CENTIMETER 46 1512

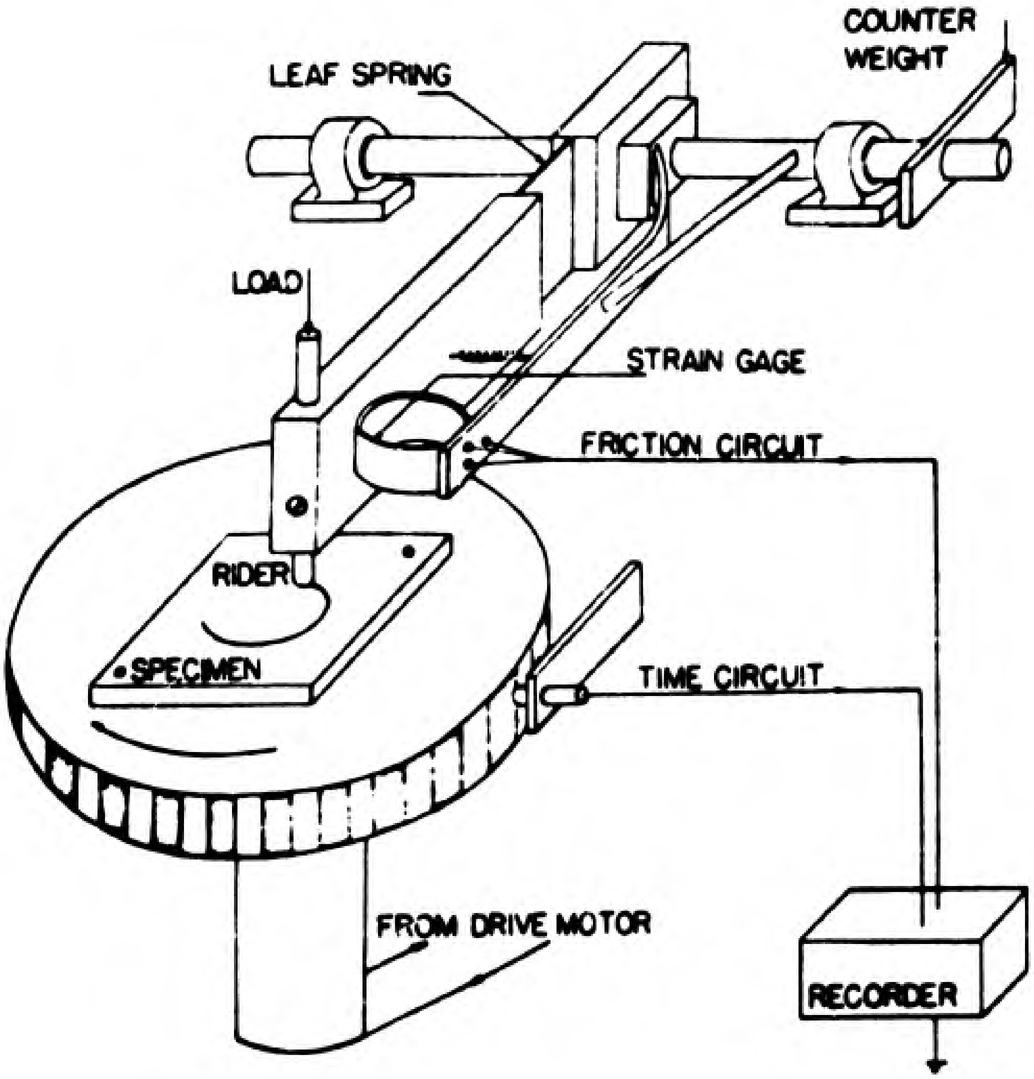

Figure 1. Schematic Illustration of the Single Rider Friction Apparatus.

ENCLOSURE 1

JET ENGINE MANUFACTURER'S ESTIMATE OF
MAINSHAFT BEARING OPERATING SPEED AND TEMPERATURE REQUIREMENTS

(DN = bearing bore diameter in mm times shaft speed in rpm)

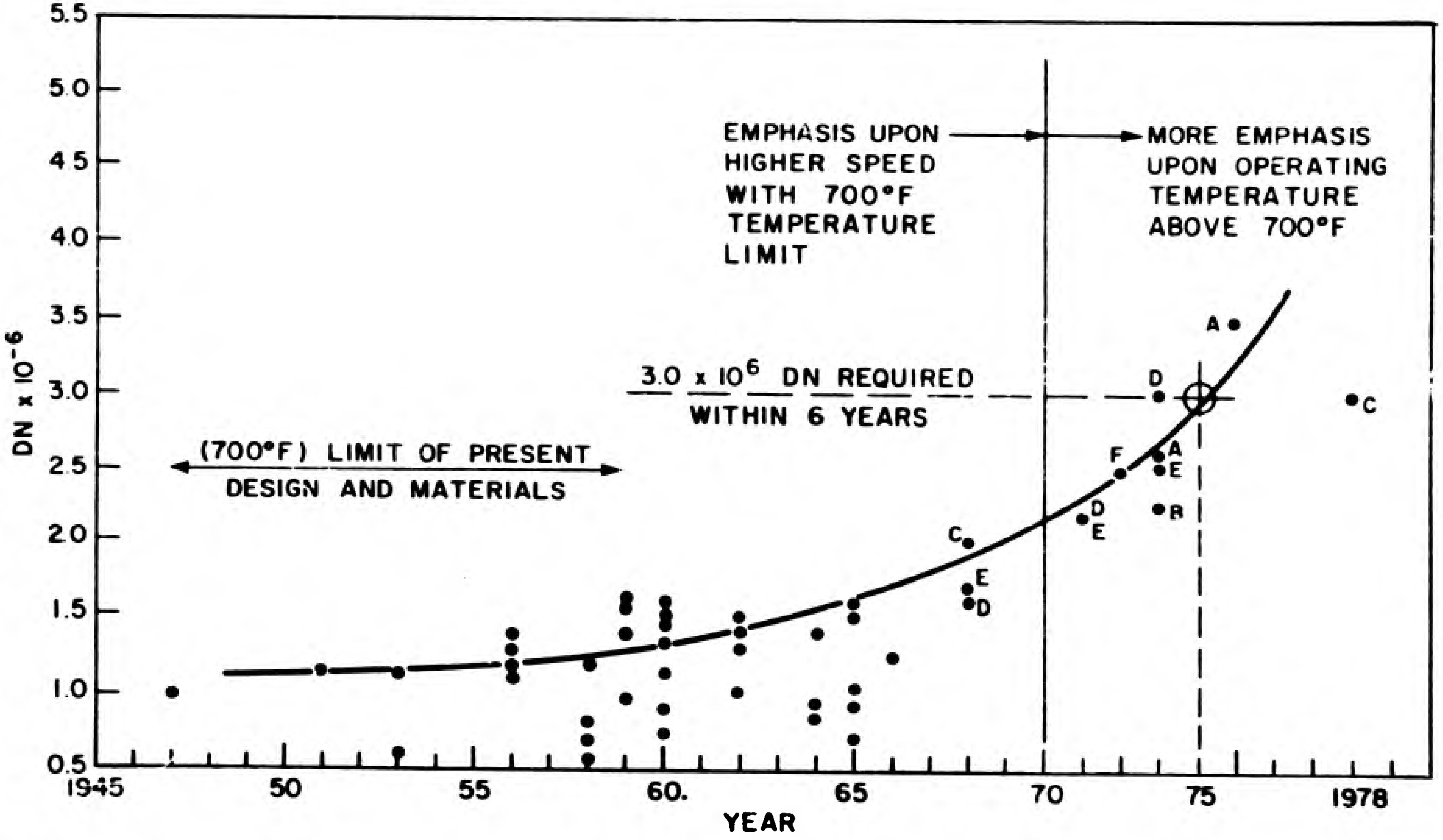

AL74P009

ENCLOSURE 2

SPECIAL 201-SIZE BALL BEARING WITH CEMENTED CARBIDE RINGS, CERAMIC BALLS AND MOLYBDENUM CAGE AFTER 12 HOURS OPERATION AT 1500°F, 8000 RPM, THRUST LOADED TO 300,000 PSI CONTACT STRESS, AND LUBRICATED WITH MoS_2 POWDER IN ARGON CARRIER.

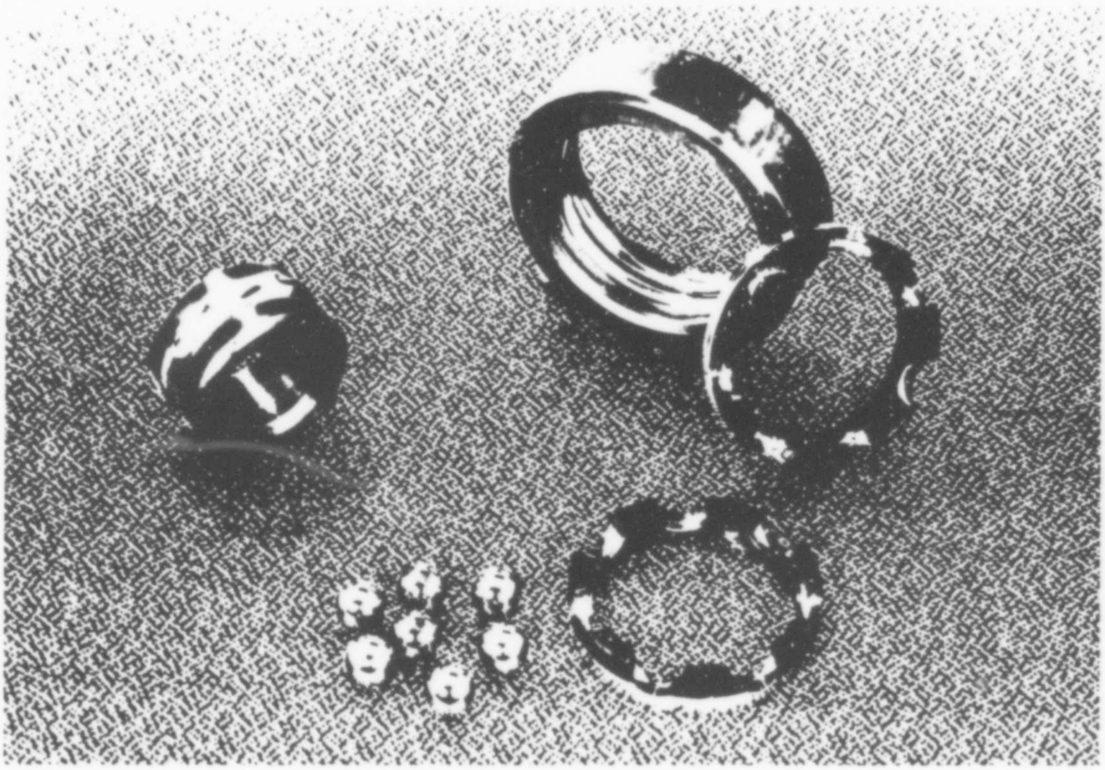

ENCLOSURE 3

COMPARISON OF PROPERTIES* OF
SILICON NITRIDE AND BEARING STEELS

Property	Silicon Nitride	52100 Steel	M50 Steel
Compressive Strength (psi)	500,000	400,000	340,000
Elastic Modulus (psi)	45×10^6	30×10^6	30×10^6
Linear Thermal Expansion $(°F)^{-1}$	1.5×10^{-6}	8×10^{-6}	8×10^{-6}
Density (g/cc)	3.18	7.89	7.89
Hardness (Rc)	80-85	60	62
Maximum Use Temp. (°F)	3,000	400	700

* Room Temperature Unless Otherwise Stated.

ENCLOSURE 4

TYPICAL PROPERTIES OF NORTON HOT PRESSED SILICON NITRIDE

1) Bulk density (g/cc)			3.2
2) Modulus of elasticity (psi)	25°C		45×10^6
	1000°C		45×10^6
3) Room Temperature compressive strength (psi)			500,000
4) Modulus of rupture (psi)	25°C		130,000
	900°C		120,000
	1300°C		75,000
5) Knoop Hardness with 100 g. load (kg/mm2)			2200
6) Linear thermal expansion in the range 25-1500°C (per °C)			2.75×10^{-6}
7) Thermal conductivity (BTU-in/hr.-ft2-°F)		25°C	116
		1000°C	70
8) Specific heat (BTU/lb-°F)		25°C	0.17
		1000°C	0.39

AL74P009

ENCLOSURE 5

Spall morphology on a Silicon Nitride ball run in a five-ball tester. 100X

ENCLOSURE 6

A halo of lube distress formed around the spall
300X

AL74P009

ENCLOSURE 7

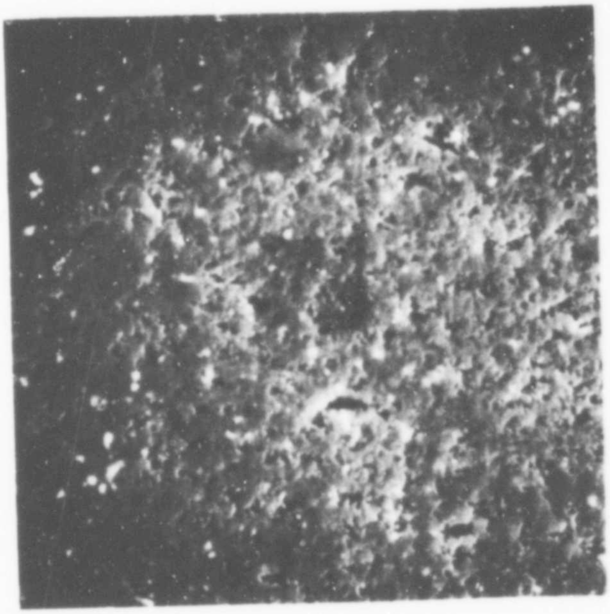

Surface of an unrun Silicon Nitride Ball as Received 1000X

ENCLOSURE 8

LIST OF TEST LUBRICANTS AND THEIR PROPERTIES

		Kinematic Viscosity c.s. (100/210°F)	Surface Tension (dyne/cm)	Sp. Wt. (100°F)	Temp. Viscosity Coefficient (β)°F^{-1}	Refractive Index (25°C)
1.	Ester Oil With Additive (Mobil Jet II)	28/5.1	30.5 (100°F)	0.987	0.0154	1.4570
2.	Synthetic Paraffinic With Additive (XRM-177F)	442/42	31.0 (25°C)	0.84	0.0216	1.4690
3.	Mineral Oil (DTE Med. Hvy.)	63.6/8.1	33.13 (100°F) 27.53 (210°F)	0.882(60°F)	0.0187	
4.	Synthetic Paraffinic (XRM-109F)	447/42.6	30.8 (25°C)	0.84	0.0214	1.4689
5.	Polyphenyl ether	346/13	47.4 (100°F)	1.195	0.297	1.6310
6.	Ester Base Oil (XRM-234)	28/5.1	30.5 (100°F)	0.987	0.0154	1.4570

AL74P009

ENCLOSURE 9

TYPICAL SILHOUETTE OF OIL DROPS ON THE SILICON NITRIDE SUBSTRATE

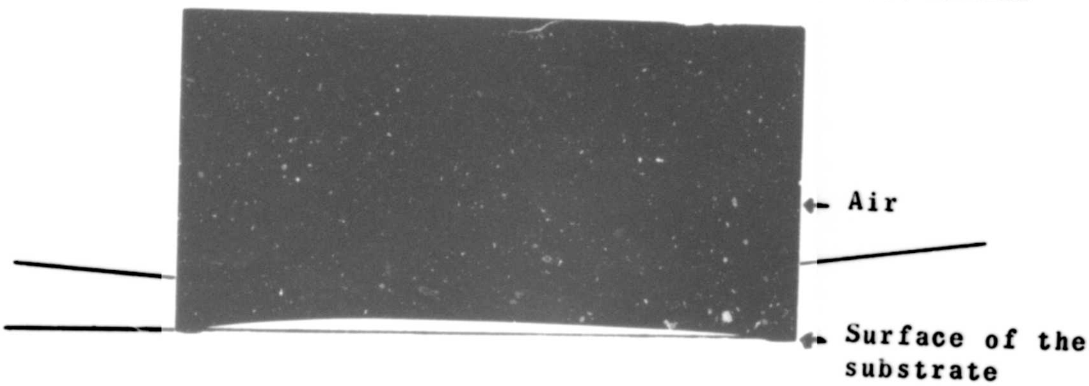

a) MIL-L-23699
(No. 1 - Table 1)

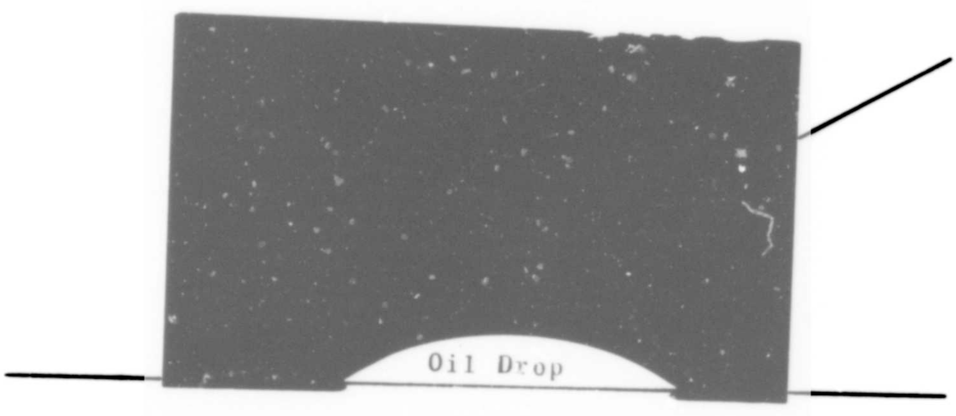

b) Polyphenyl ether
(No.5 - Table 1)

ENCLOSURE 10

RESULTS OF CONTACT ANGLE MEASUREMENTS

No.	Oil	Surface Roughness, μ in. 15	15	1.5
		Contact Angle (Perpendicular to lay)	(Parallel to lay)	(Isotropic)
1	Mobil Jet II (MIL-L-23699)	10°	6°	5°
2	XRM 177 F	18°	6°	16°
3	DTE Medium Heavy	5°	4°	15°
4	XRM 109 F	17°	12°	13°
5	OS 124	37°	29°	29°
6	XRM 234	26°	11°	6°

ENCLOSURE 11

SCHEMATIC OF OPTICAL EHD TEST RIG

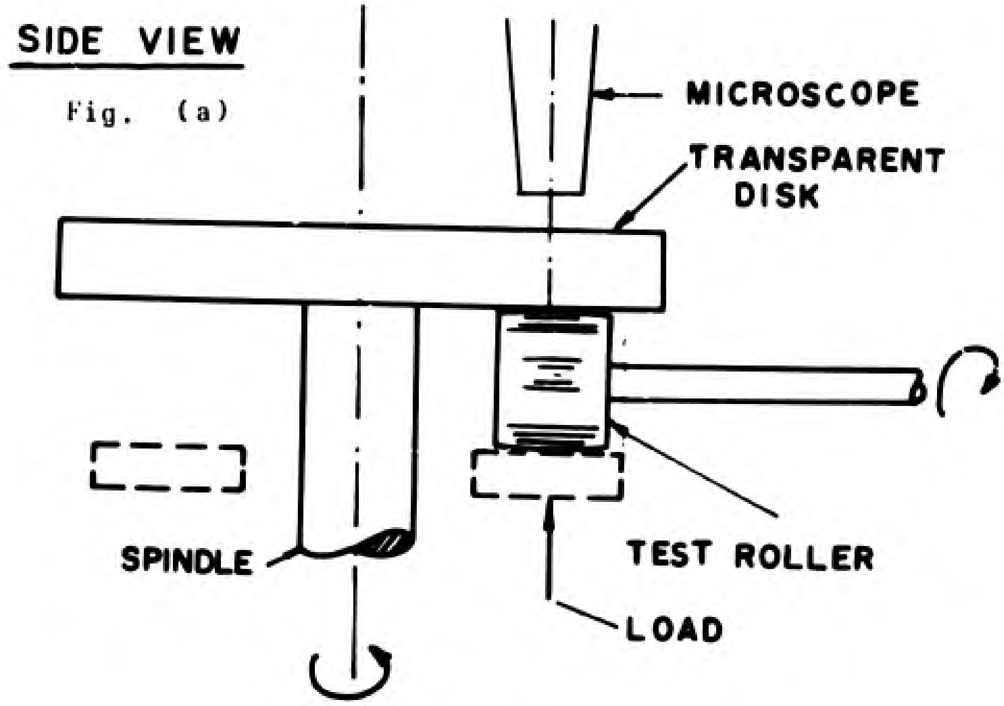

Fig. (a)

BASIC TEST CONFIGURATION

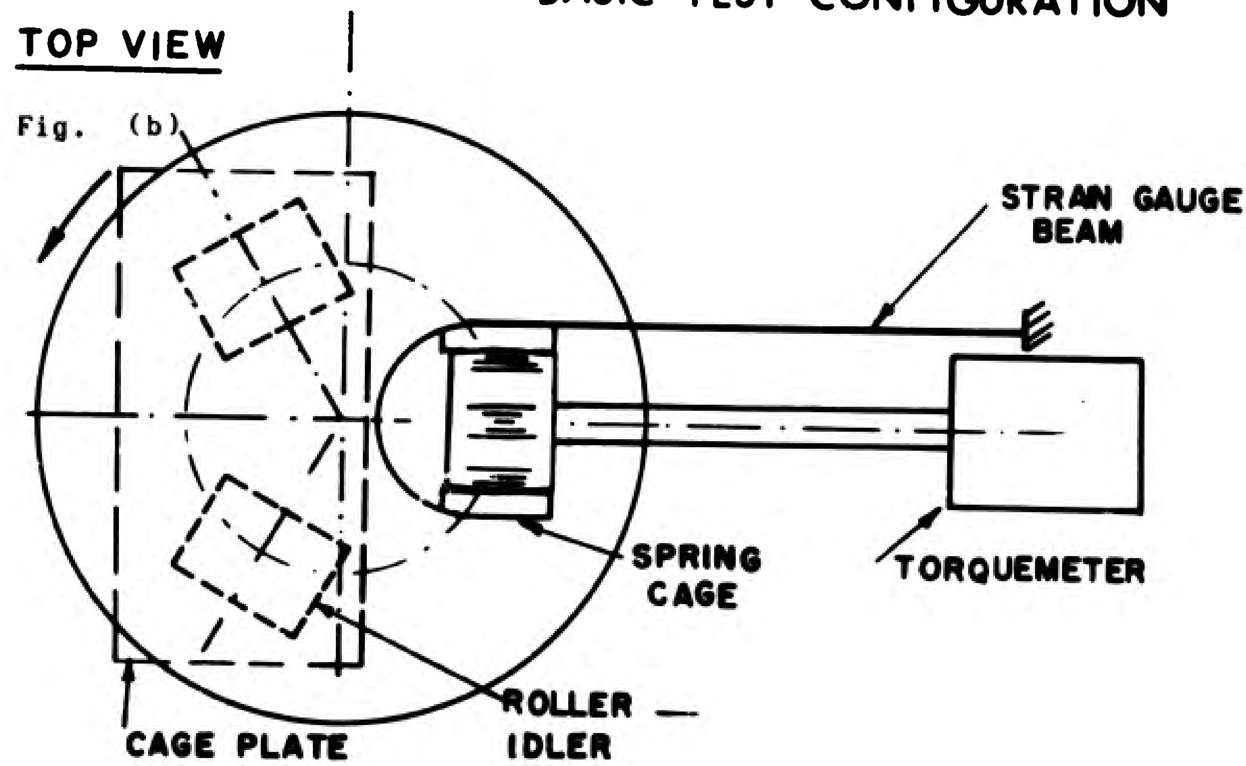

Fig. (b)

AL74P009

ENCLOSURE 12

EHD TEST RIG ASSEMBLY

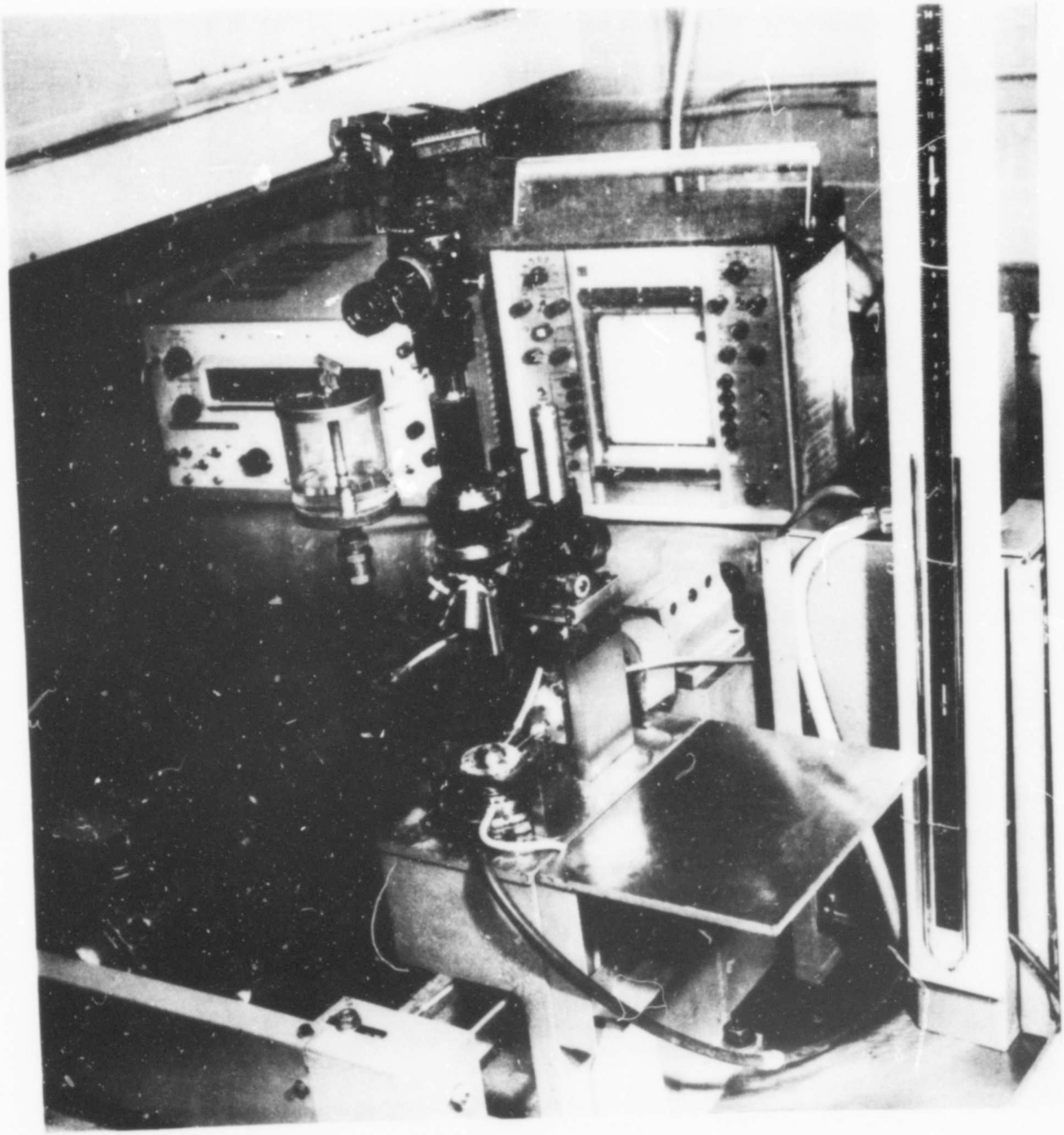

RESEARCH LABORATORY SKF INDUSTRIES, INC.

ENCLOSURE 13

EHD TEST RIG OPTICAL SYSTEM

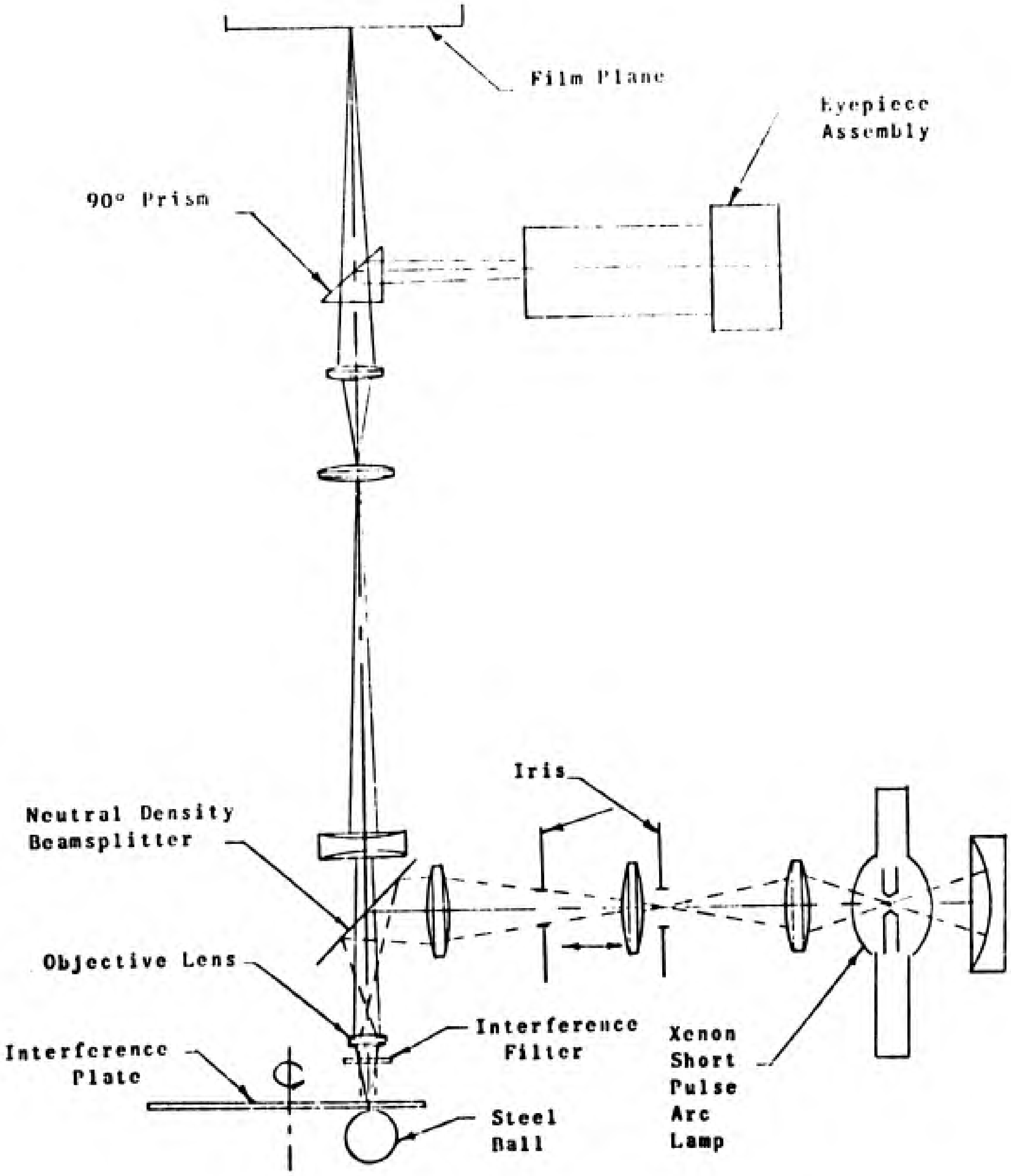

ENCLOSURE 14

ASTM Standard Temperature-Viscosity Chart for the Six Oils Used in this Program.

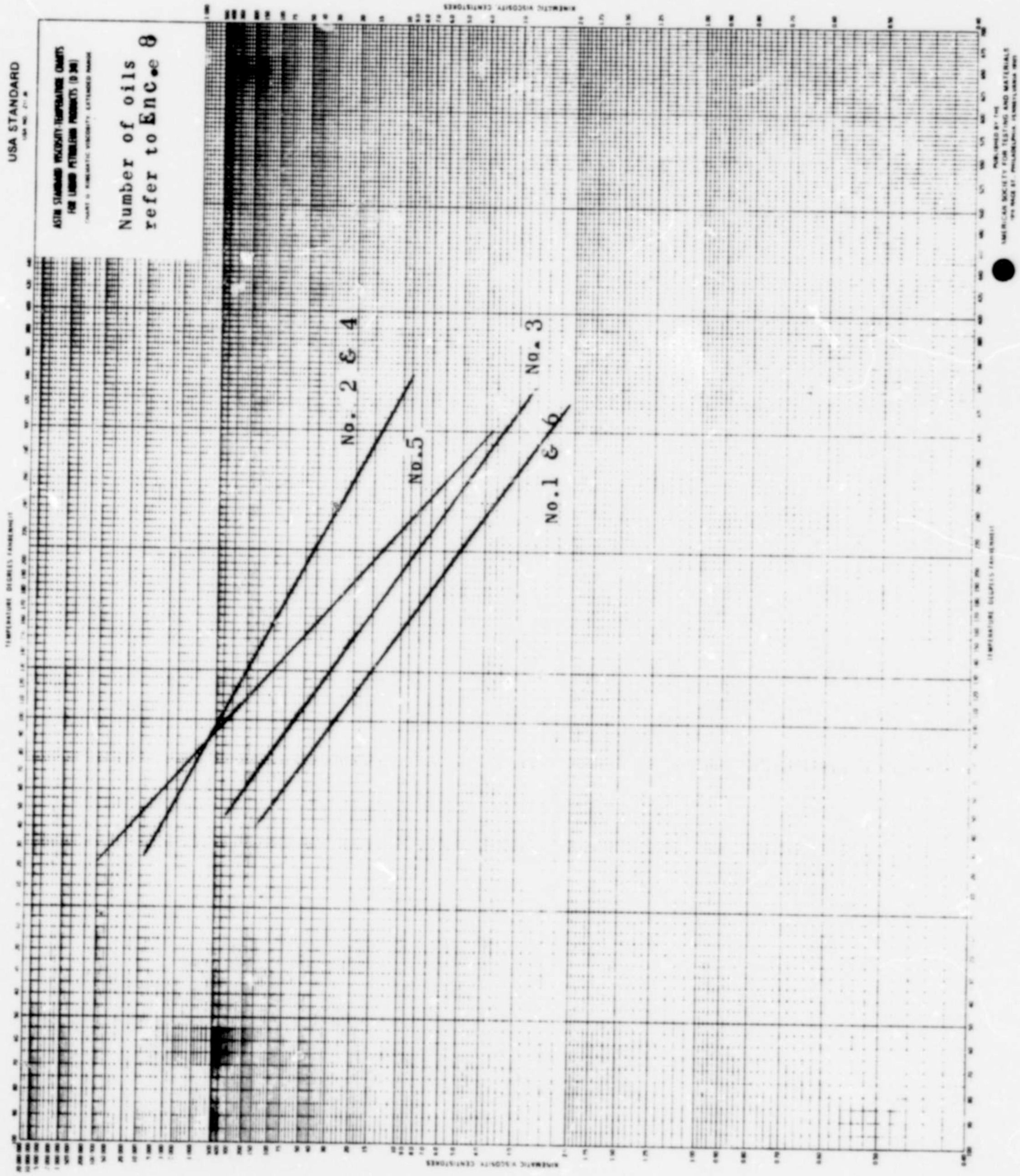

ENCLOSURE 15

FRINGE PHOTOGRAPHS OF EHD CONTACTS WITH STARVATION

Lubricant: Ester Oil (MIL-L-23699)
Speed: 40 in/sec
52100 steel ball

Exit Inlet

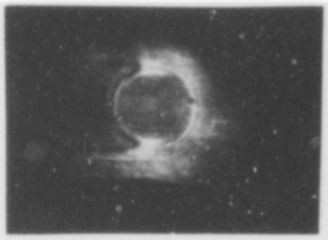

Sapphire - Steel Contact
Po = 305 ksi

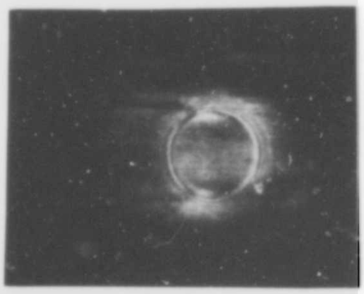

Glass - Steel Contact
PO = 126 ksi

ENCLOSURE 16

FILM THICKNESS AS A FUNCTION OF INTERFERENCE COLOR FOR XENON AND INCANDESCENT LIGHT SOURCES

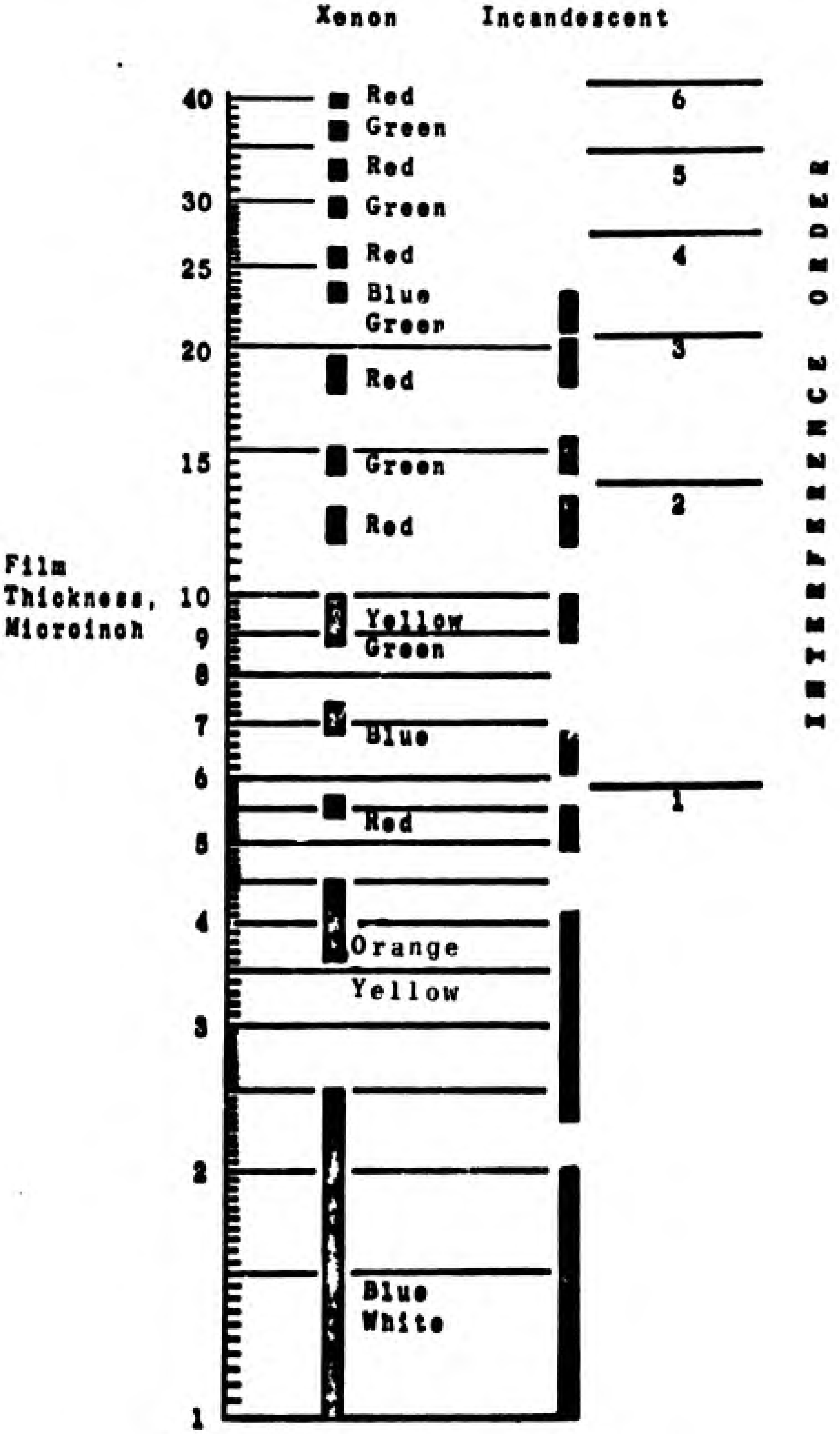

ENCLOSURE 17

VARIATION OF REFRACTIVE INDEX WITH PRESSURE

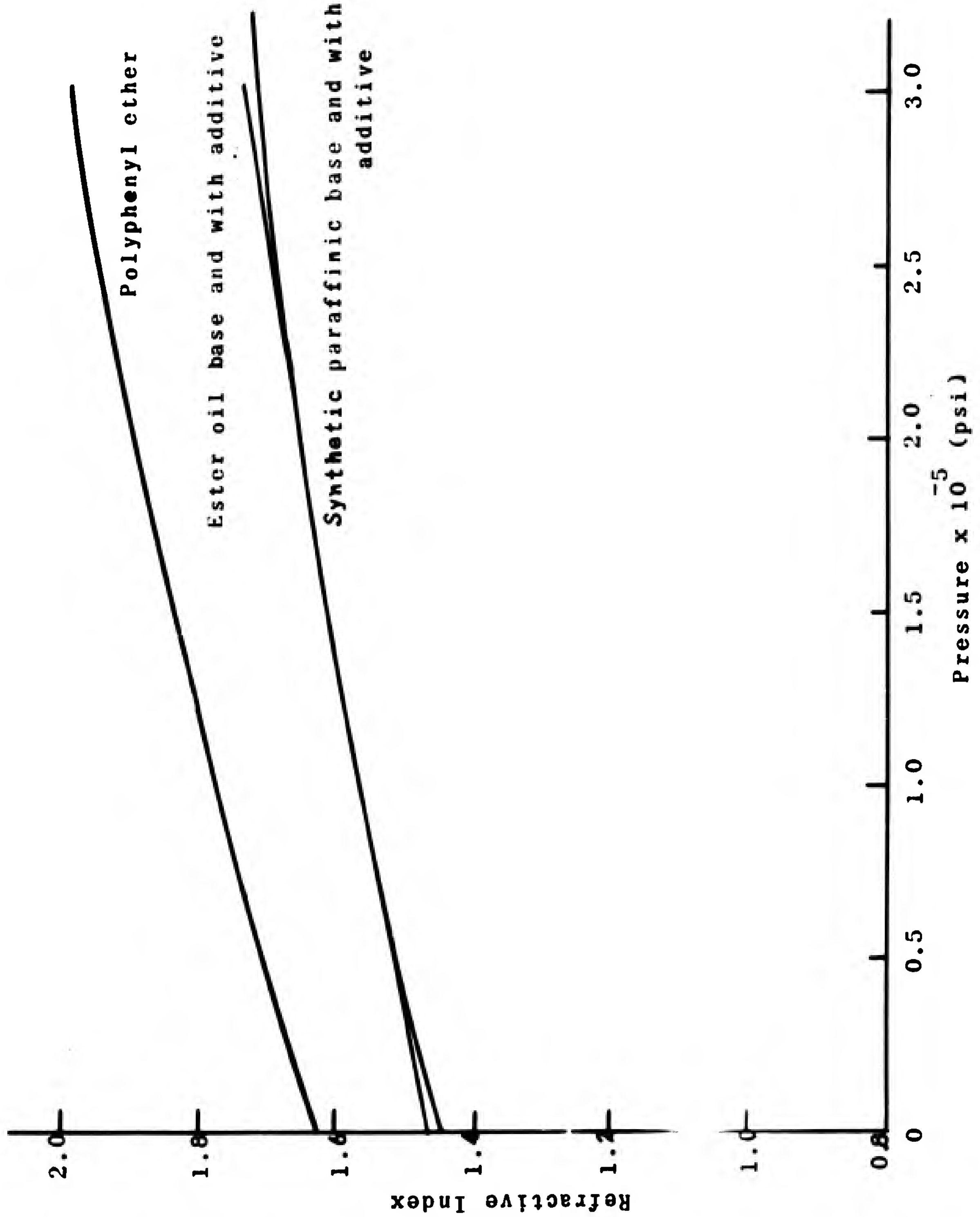

ENCLOSURE 18

SURFACE OF AN UNRUN SILICON NITRIDE BALL AFTER FERRIC OXIDE POLISHING

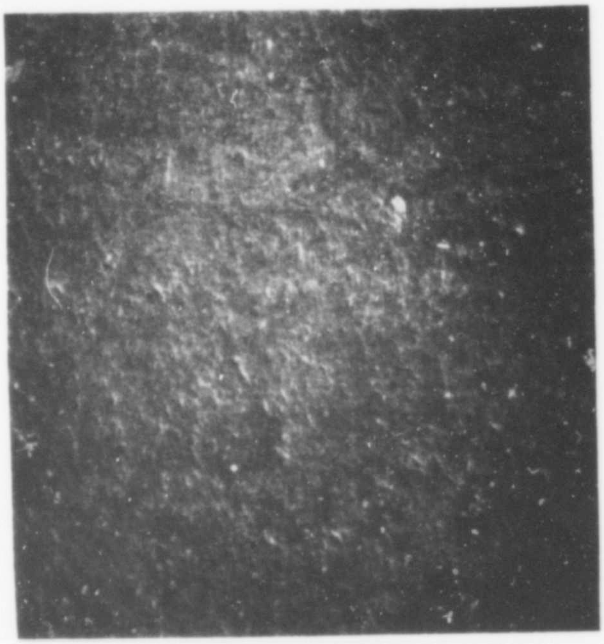

a) 1000X

b) 3000X

AL74P009

ENCLOSURE 19

STATIC FRINGE PHOTOGRAPH OF POLISHED SILICON NITRIDE BALL IN OPTICAL EHD RIG

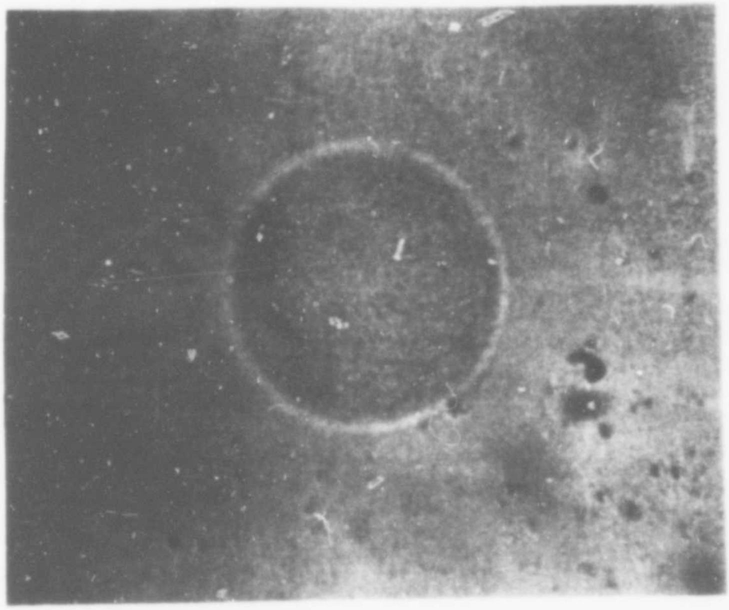

AL74 P009

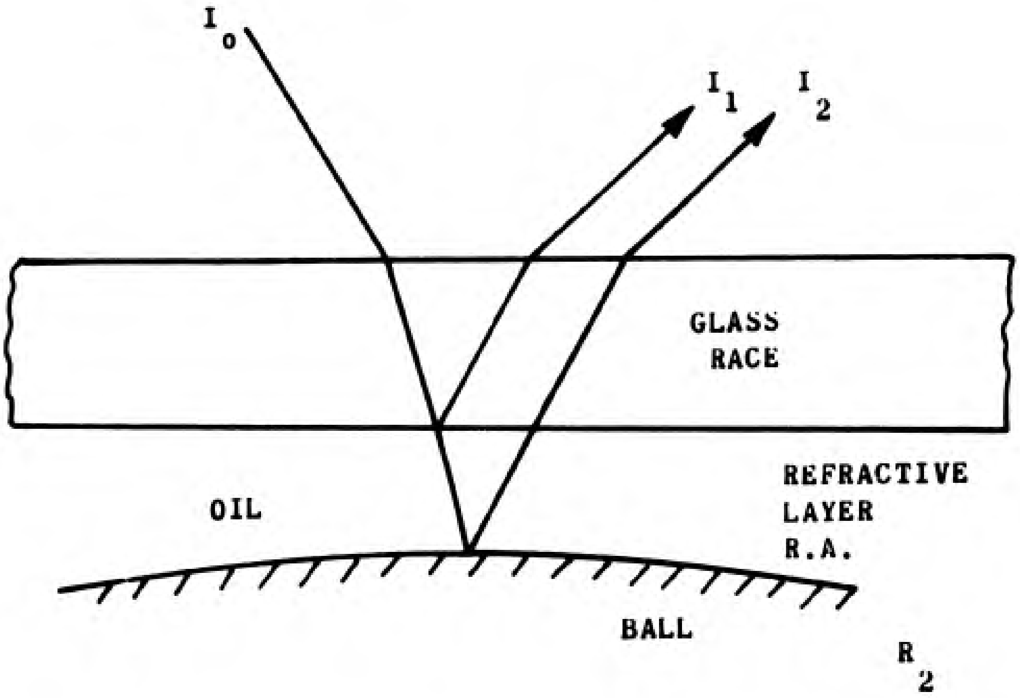

Optical Path of Light Beam Reflected From
Coated Glass Plate and the Ball Surface.

ENCLOSURE 21

PROPERTIES OF COATINGS

Coating Material	Reflectivity (%)	Absorption (%)
CeO	25	0.5
Ce O	20	0.5
SiO	20	10

ENCLOSURE 22

CALCULATED FRINGE VISIBILITIES FOR VARIOUS COMBINATIONS OF BALL AND COATING MATERIALS

Materials		Reflectivity		Absorption	Relative Beam Intensity		Interference Fringe Visibility
Ball	Layer	R_2 (Ball)	R_1 (Layer)	A_1 (Layer)	I_1/I_0	I_2/I_0	V
Steel	CeO	60%	30%	0.5%	0.30	0.27	0.9986
Si_3N_4	CeO (1)	40%	30%	0.5%	0.30	0.195	0.9772
Si_3N_4	CeO (2)	40%	25%	0.5%	0.25	0.224	0.9984
Si_3N_4	CeO (3)	40%	20%	0.5%	0.20	0.256	0.9924
Si_3N_4	SiO	40%	20%	10%	0.20	0.196	0.9999

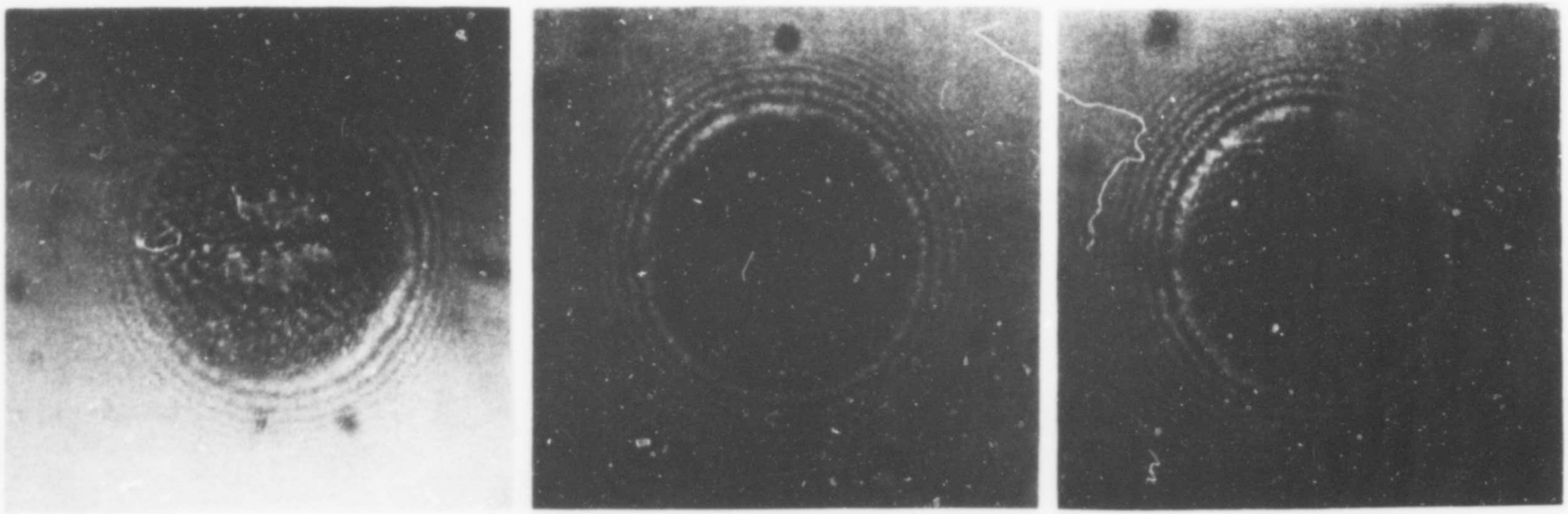

(a) (b) (c)

	(a)	(b)	(c)
Coating:	C_eO	C_eO	S_iO
Reflectivity (%):	25	20	20
Absorption (%):	0.5	0.5	10

Enclosure 23. Comparison of Static Fringegrams Obtained at 5 lbs. Load.

Exit  Inlet

Enclosure 24. Dynamic Fringegram of a Silicon Nitride-Glass Contact.

Speed = 40 in/sec. Max. Hertz Stress = 113 ksi.
Lubricant: Mobil Jet II

ENCLOSURE 25

Variation in Measured Film Thickness with Rolling Speed at Two Loads (5 and 15 lbs.) for Si_3N_4 and Steel.

Lubricant: Mobil Jet II
Coating: SiO 25% Reflectivity

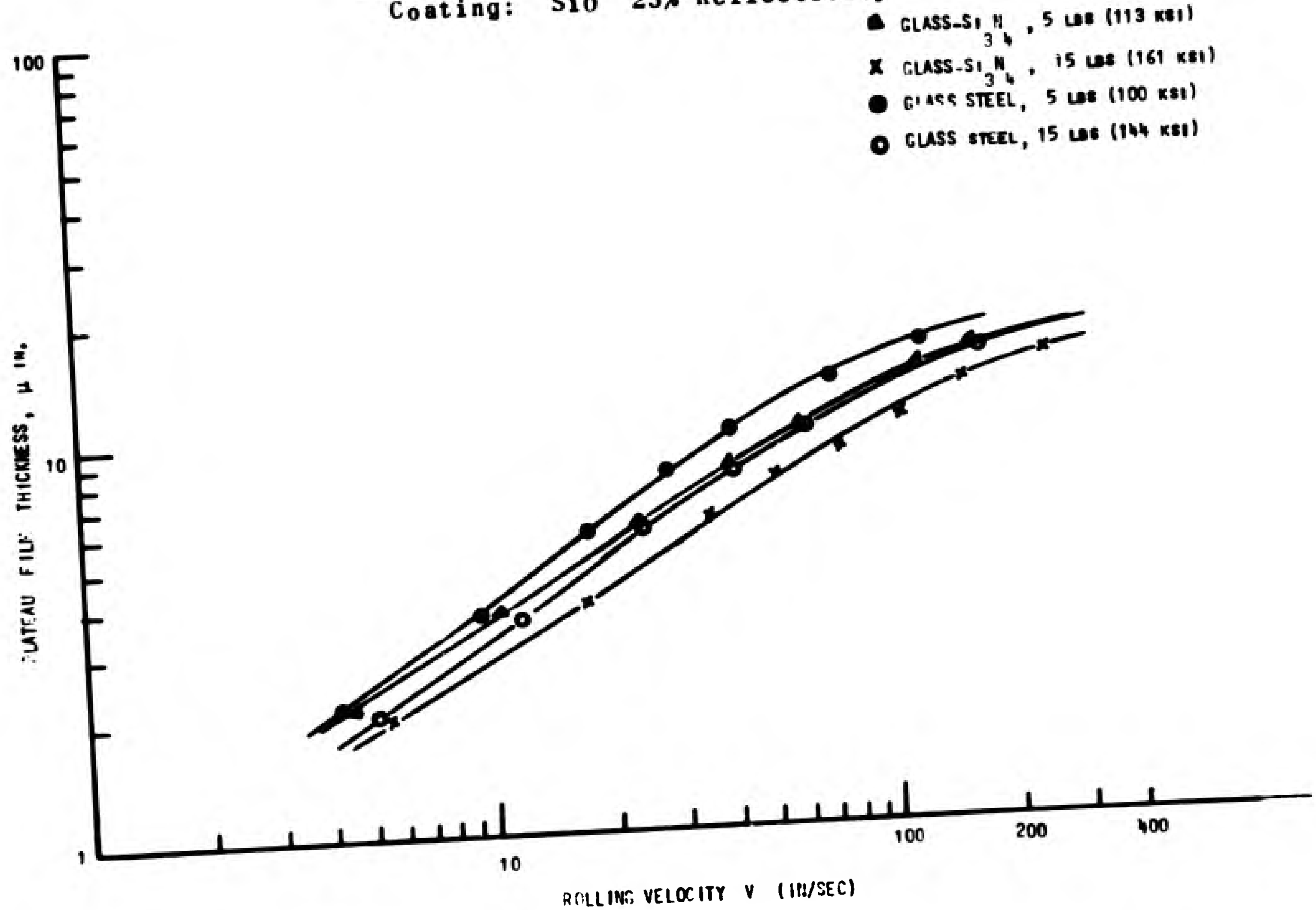

AL74P009

ENCLOSURE 26

Variation with Rolling Speed of the Ratio of Measured Film Thickness to the Theoretical Unstarved Film Thickness (hof).

Lubricant: Mobil Jet II

Coating: SiO 25% Reflectivity

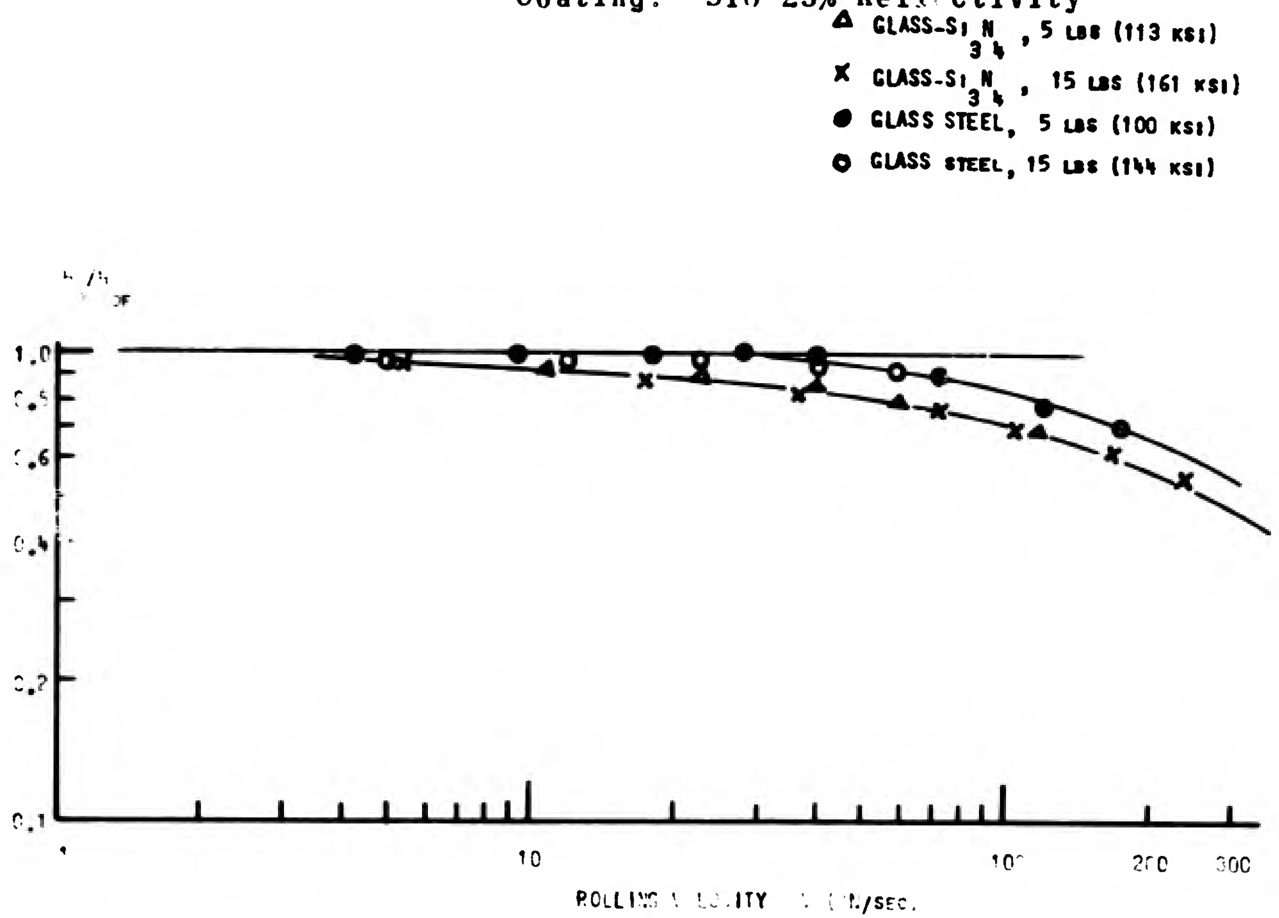

AL73P017

Color Fringegrams of Si_3N_4-Glass Contacts at Loads = 5 and 15 lbs. and Three Speeds for Each Load.


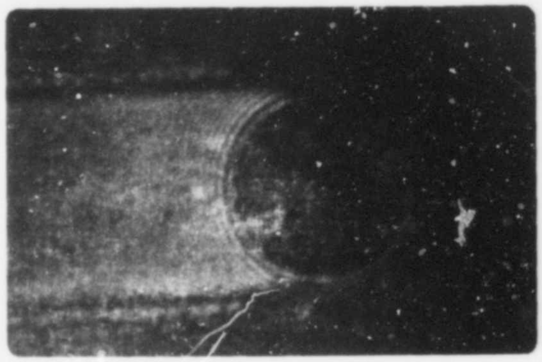

Q = 5 lbs. V = 20 in/sec. D   A Q = 15 lbs. V = 5 in/sec.

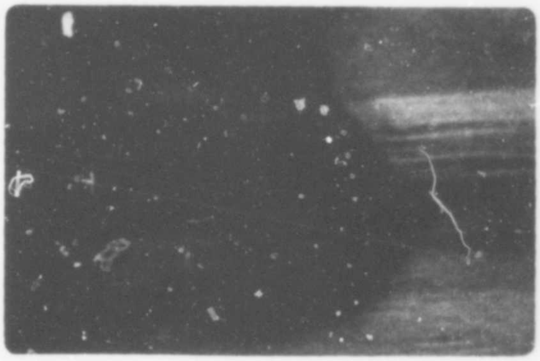
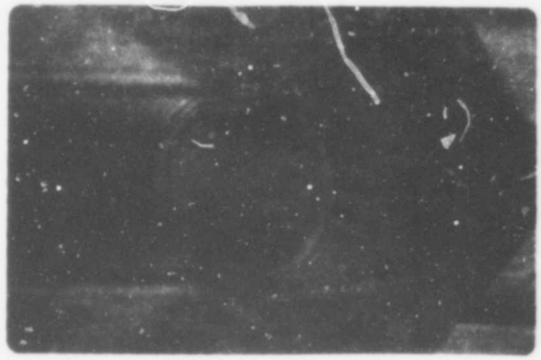

Q = 5 lbs. V = 100 in/sec. E   B Q = 15 lbs. V = 60 in/sec.

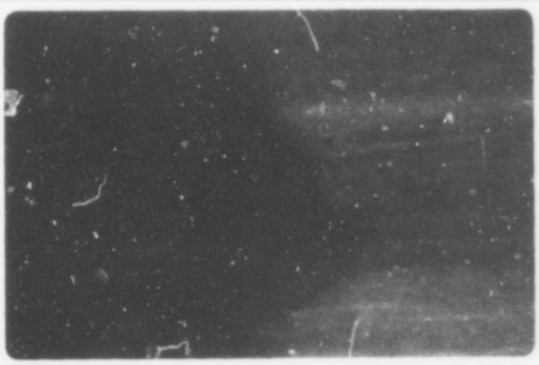
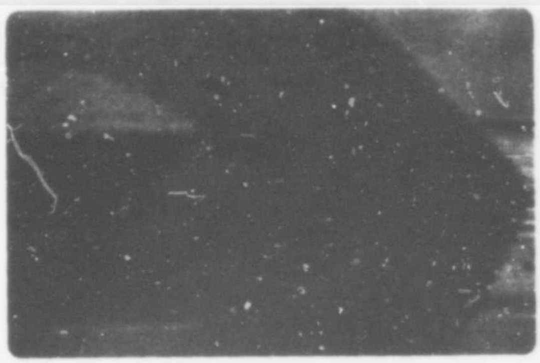

Q = 5 lbs. V = 200 in/sec. F   C Q = 15 lbs. V = 100 in/sec.

AL74P009

ENCLOSURE 28

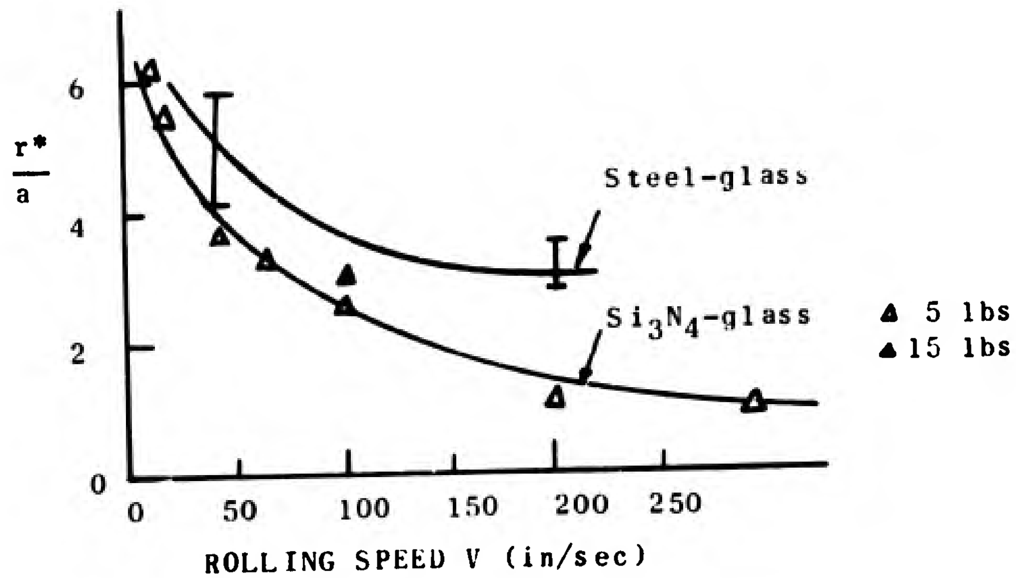

Distance of Contact Center of the Meniscus (r*) Scaled by the Hertz Contact Radius (a) as a Function of Rolling Speed (V).
Lubricant: Mobil Jet II

Traction Curves for Oil No. 6
(Ester Base Oil)

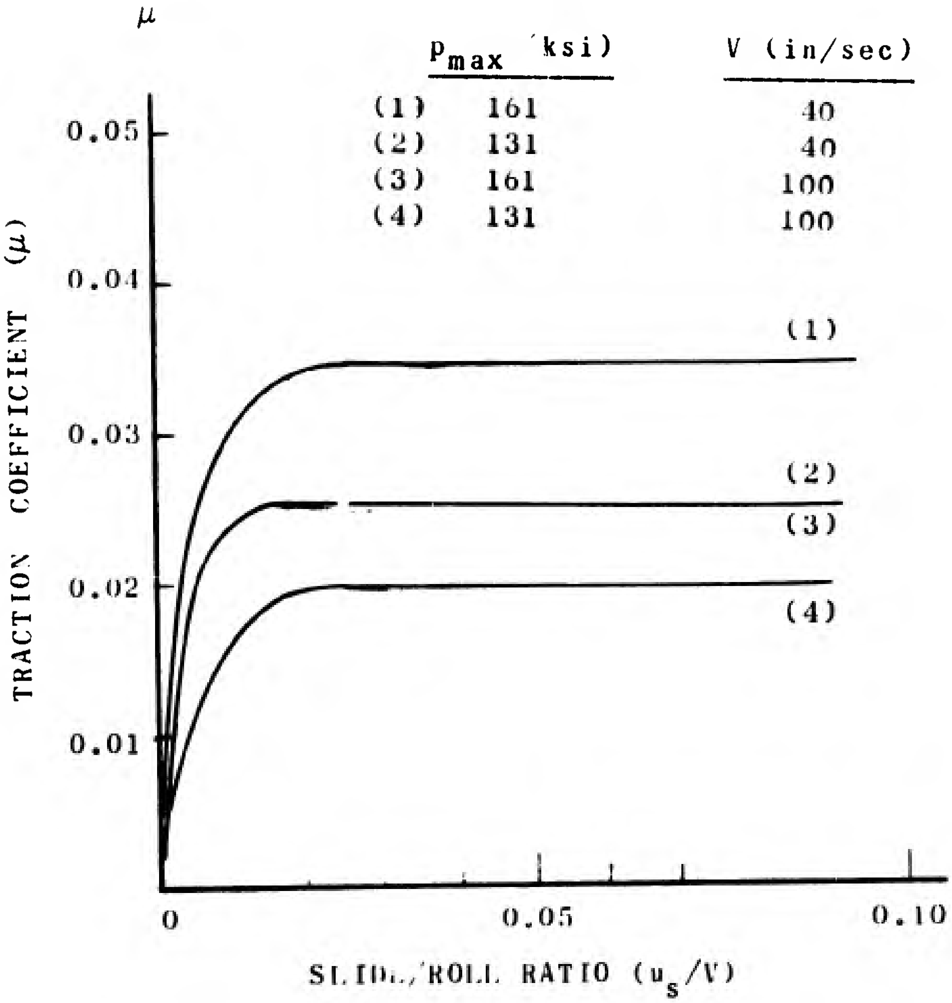

ENCLOSURE 30

MAXIMUM TRACTION COEFFICIENTS OF SIX TEST OILS

Material: Silicon Nitride-Glass, Axis Ratio 1:1

Oil	Maximum Stress (ksi)	Rolling Speed 40 in/sec (90°F)	Rolling Speed 100 in/sec (100°F)	Rolling Speed 400 in/sec (113°F)
Synthetic paraffinic	113	0.0161	0.010	-
	141	0.0168	0.0093	0.0085
	163	0.026	0.0172	0.0077
Synthetic Paraffinic with additive	113	0.0140	0.0126	0.0090
	141	0.0181	0.0094	0.007
	163	0.0275	0.0225	0.0154
Ester oil with additive	113	0.0186	0.0143	-
	141	0.0358	0.0240	0.0150
	163	0.0362	0.0292	0.0203
Ester base oil	113	0.0256	0.0197	0.0127
	141	0.0294	0.0222	0.0145
	163	0.0346	0.0251	0.0224
Mineral oil (DTE Med. Hvy)	113	0.0434	0.032	0.0134
	141	0.0445	0.033	0.0217
	163	0.0467	0.0388	0.0243
Polyphenyl ether	113	0.0376	0.034	0.0187
	141	0.038	0.0306	0.0290

186A

ENCLOSURE 31

TRACTION FORCE DATA FOR STEEL/SILICON NITRIDE AND STEEL/STEEL CONTACTS

Rolling Speed (in/sec)	Pmax =	216 ksi		247 ksi		271 ksi	
	Material:	St.-St.	St.-Si_3N_4	St.-St.	St.-Si_3N_4	St.-St.	Si_3N_4-St.
	Load (lbs):	10	6.95	15	10.4	20	13.9
40		0.040	0.0436	0.0455	0.0515	0.055	0.0533
100		0.031	0.0418	0.0371	0.0419	0.014	0.0474
200			0.0361	0.030	0.035	0.0375	0.0377

AL74P009

AL74P009

ENCLOSURE 32
Traction Coefficient Versus Maximum Contact Pressure

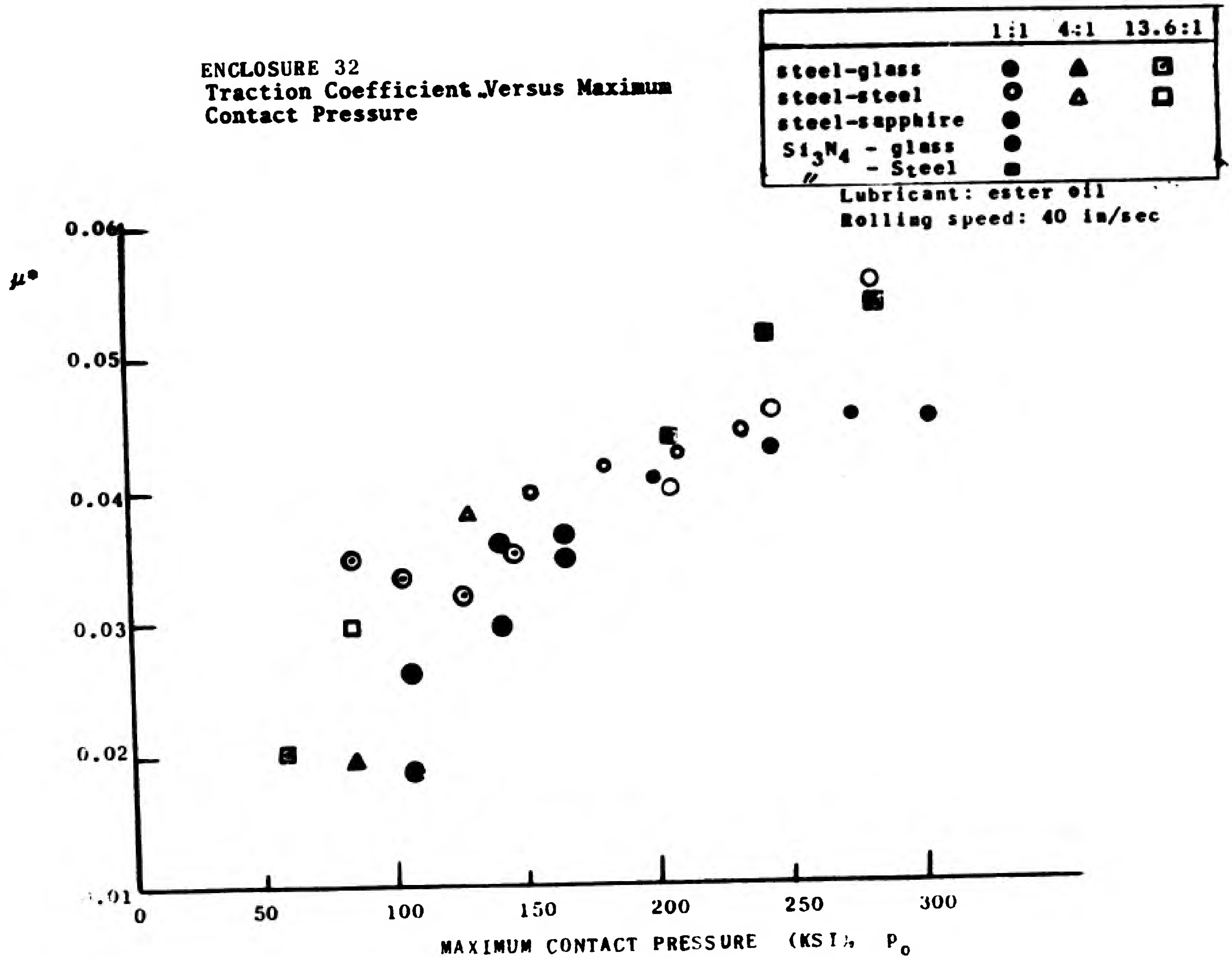

ENCLOSURE 33

AL74P009

FLAT WASHER TESTER ASSEMBLY DRAWING

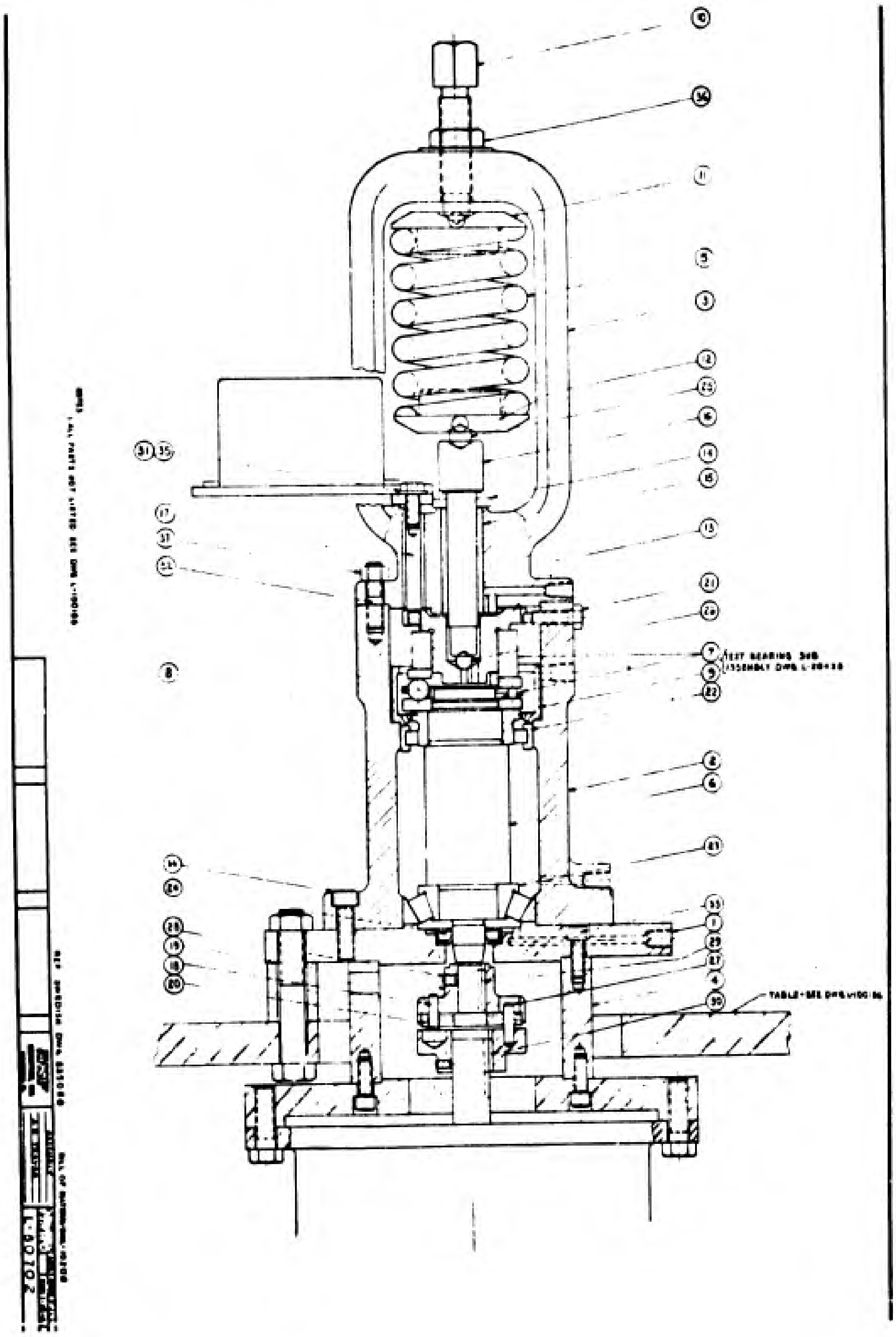

ENCLOSURE 34

TEST HEAD ASSEMBLY FOR ROLLER/FLAT WASHER MACHINE

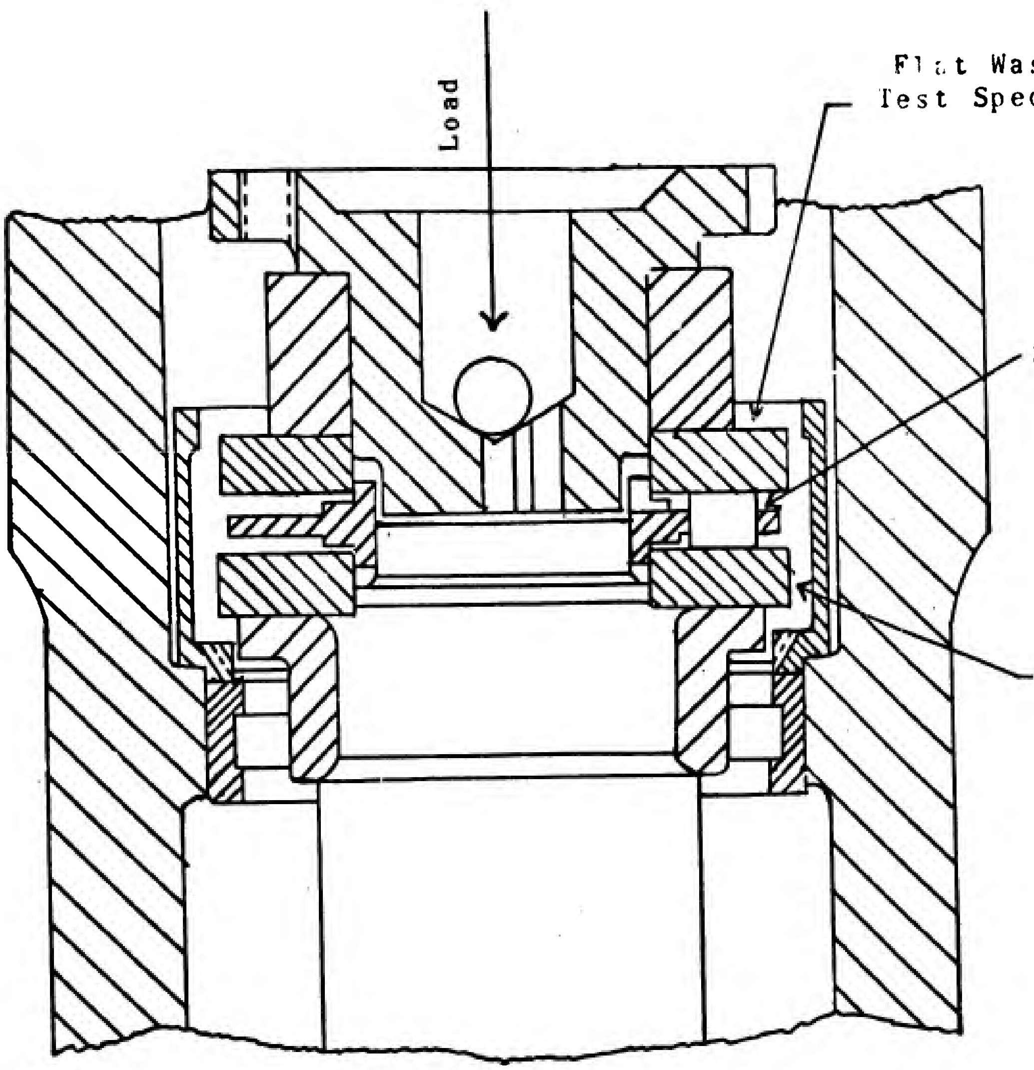

ENCLOSURE 35

DIAGRAM OF CROWNED ROLLER

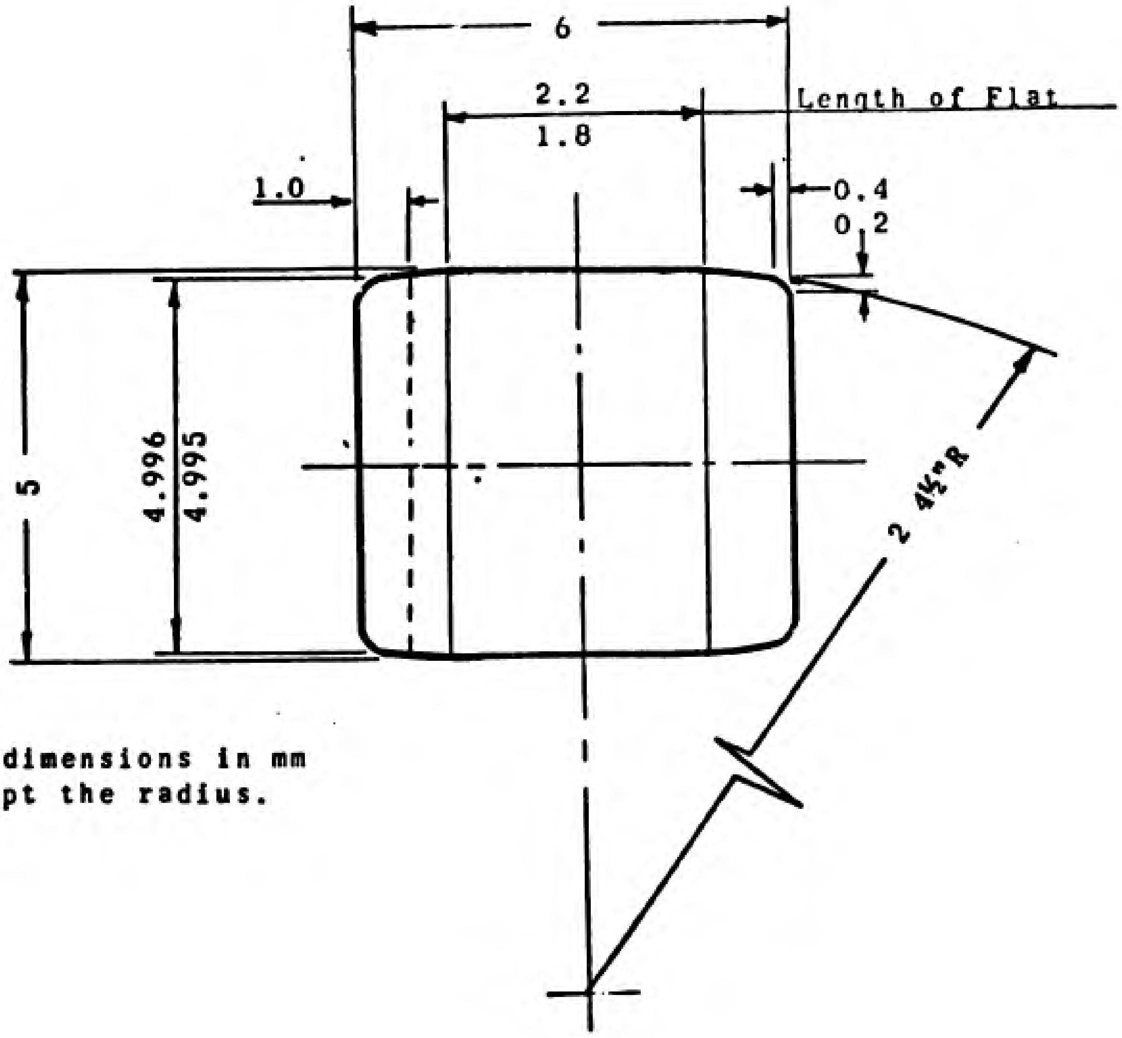

All dimensions in mm
except the radius.

ENCLOSURE 36

SILICON NITRIDE FLAT WASHER SPECIMEN DESIGN

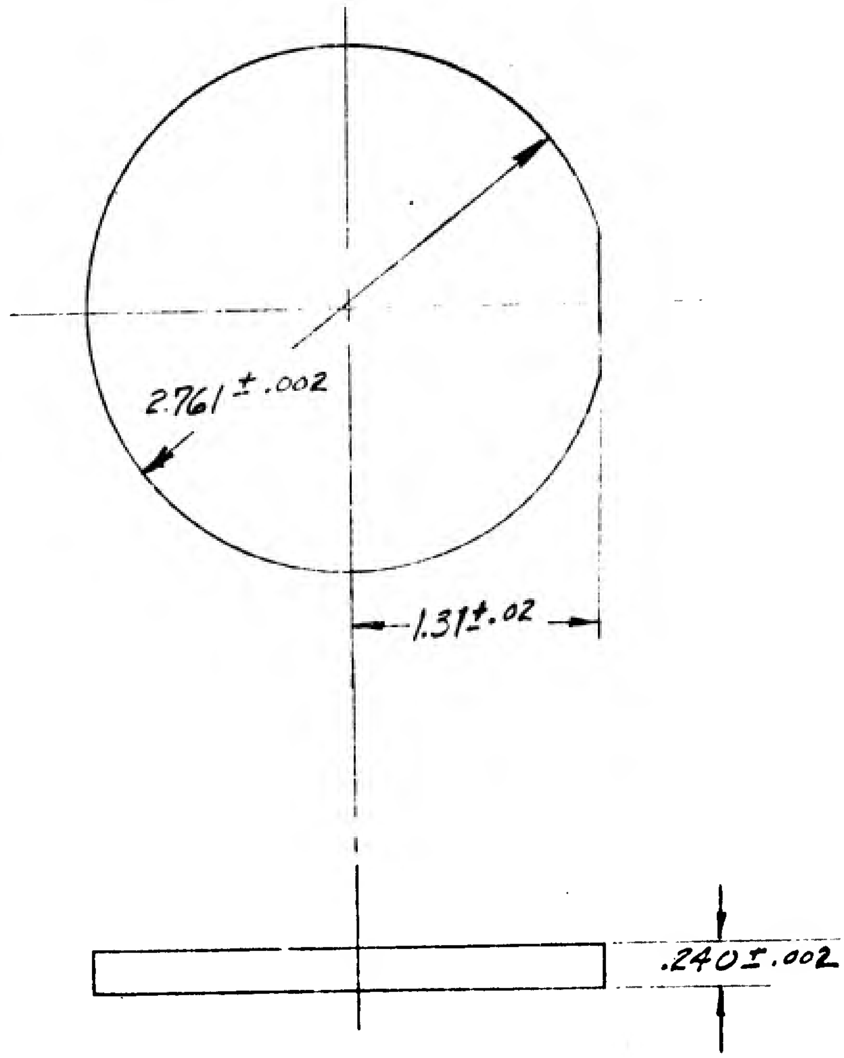

NOTES:

FACES TO BE BLANCHARD GROUND PARALLEL WITHIN .001 TIR TO SMOOTHEST POSSIBLE FINISH

ENCLOSURE 37

PHOTOGRAPH OF SEVERAL FLAT WASHER ROLLING CONTACT FATIGUE TESTERS

ENCLOSURE 38

LOAD-LIFE TESTS OF STEEL BALLS AND FLAT WASHERS OF DIFFERENT HARDNESS

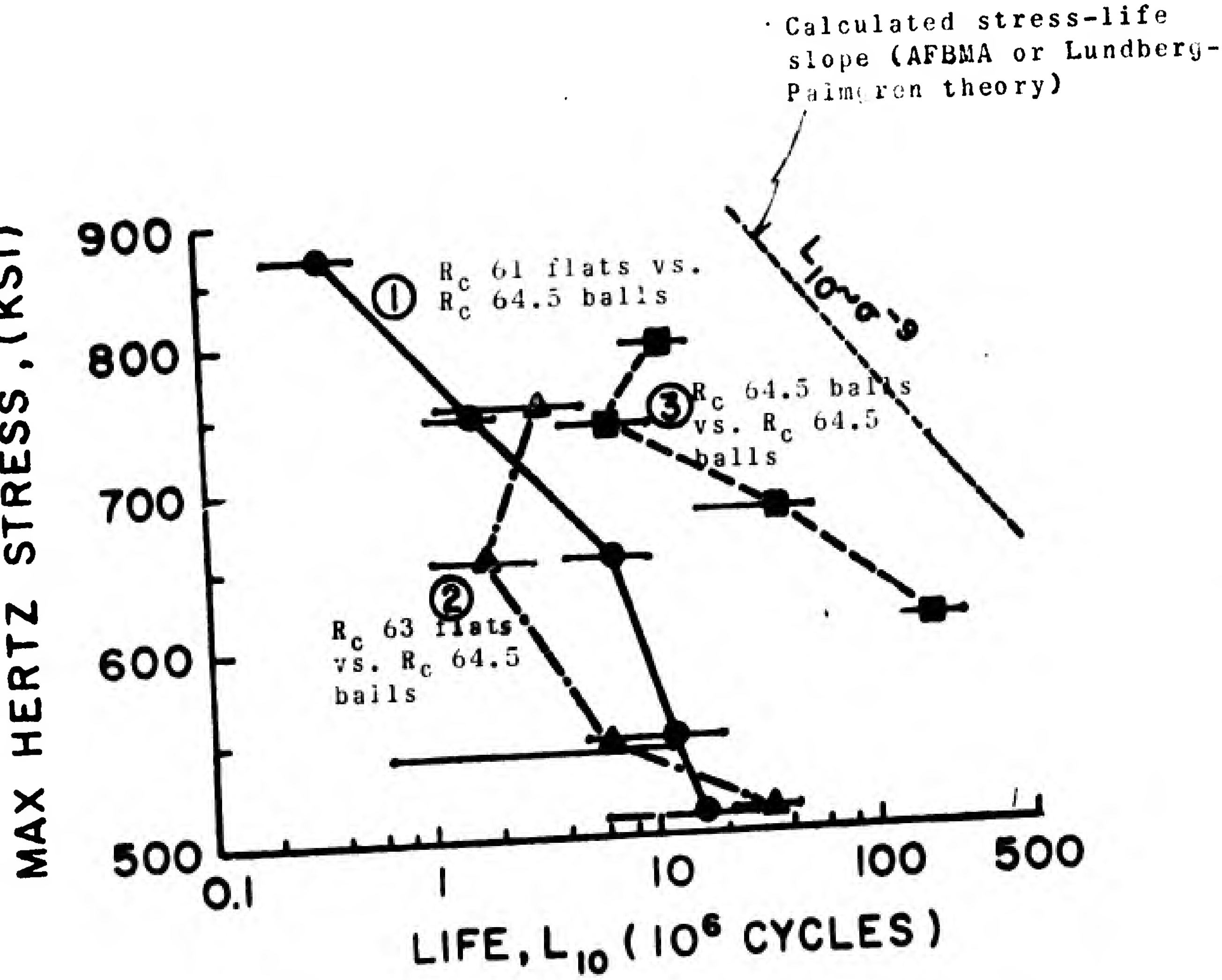

ENCLOSURE 39

LOAD-LIFE TESTS OF 61 Rc FLAT WASHERS WITH ROLLERS

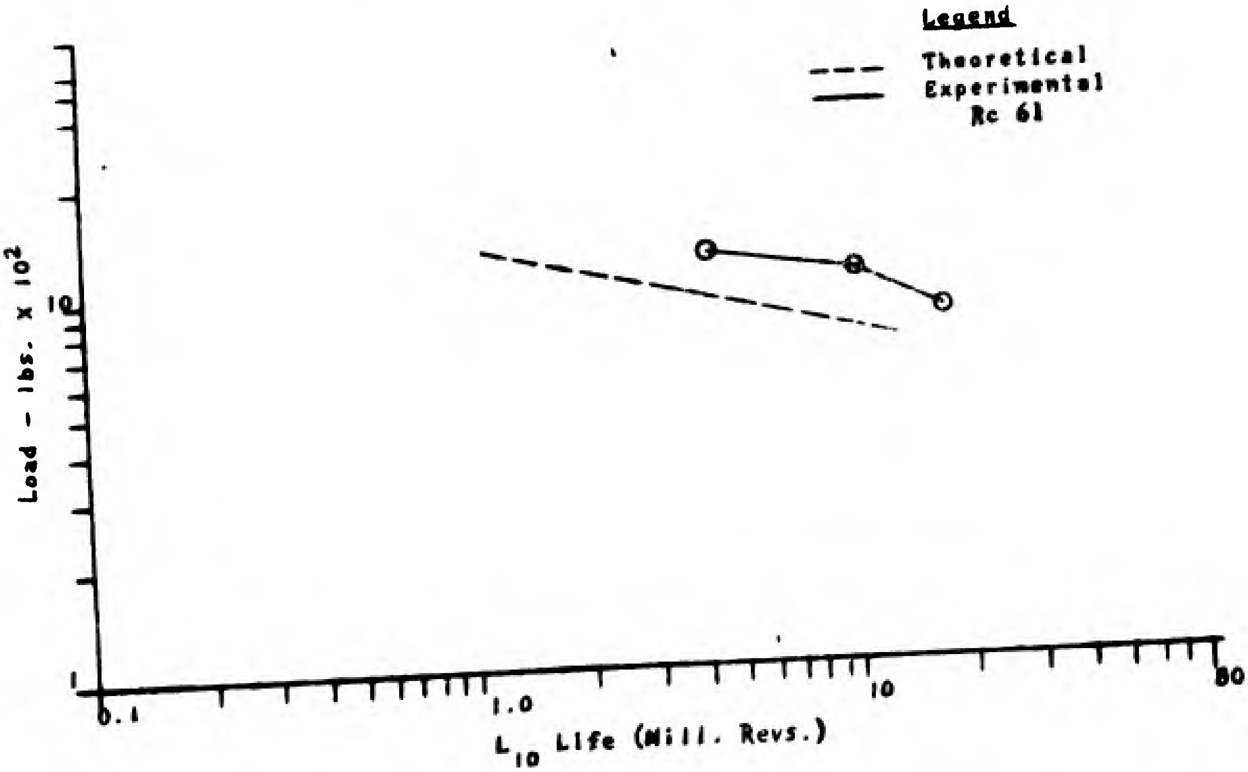

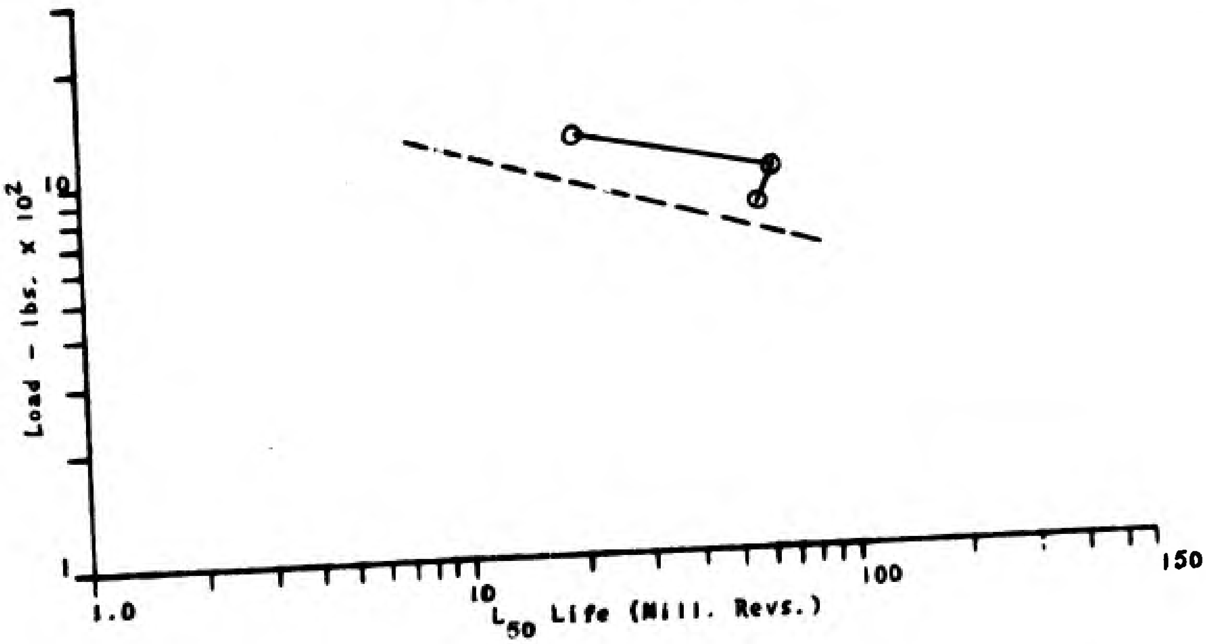

ENCLOSURE 40

TEST CONDITIONS AND RESULTS OF FLAT WASHER TESTS

Test No.	Flat Washer Bottom	Flat Washer Top	Rollers	Operating Temp. (°F)	Lubricant	Lubricant Feed Rate (drops/min.)	Load (lbs.)	Life hrs.	Life mill. revs.	Remarks
1	52100	52100	M50	235	MIL-L-23699	30	1000	4.9	0.90	1 Roller spalled
2	52100	52100	M50	170	MIL-L-23699	30	1000	12.4	2.50	2 Rollers spalled
3	Si_3N_4+	52100	M50	205	MIL-L-23699	30	500	11.3	2.20	Rollers distressed
4	Si_3N_4+	52100	M50	230	MIL-L-23699	30	1000	2.3	0.50	1 Roller spalled
5	Si_3N_4+	52100	M50	250	MIL-L-23699	30	1000	1.25	0.25	1 Roller spalled
6	Si_3N_4+	52100	Rex 49	295	MIL-L-23699	30	1000	4.0	0.80	Rollers distressed
7	Si_3N_4+	52100	Rex 49	275	MIL-L-23699	30	1000	7.25	1.45	1 Roller spalled

+As ground surface finish = 5 μ·in. AA.

ENCLOSURE 41

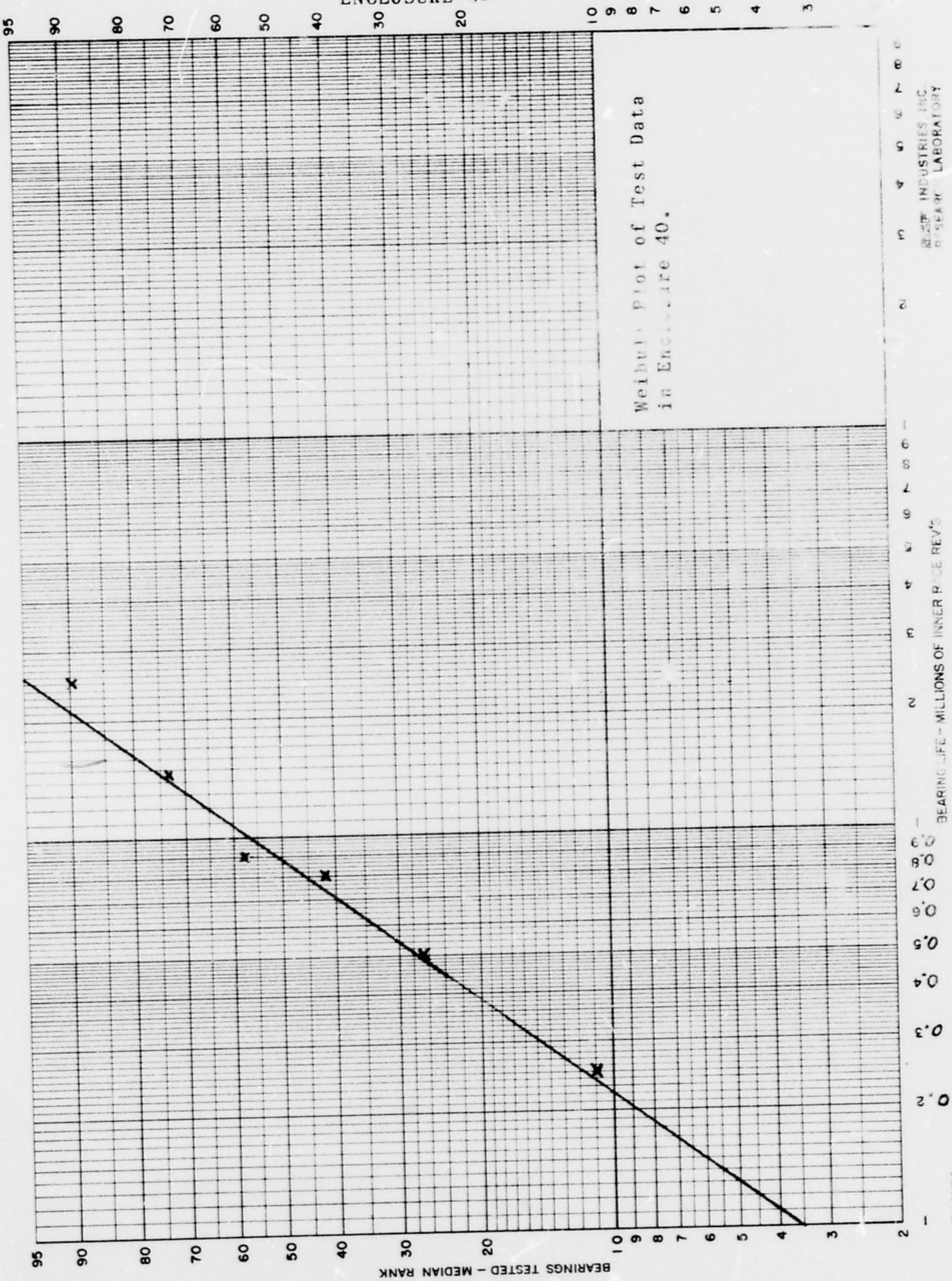

RESEARCH LABORATORY SKF INDUSTRIES, INC.

ENCLOSURE 42

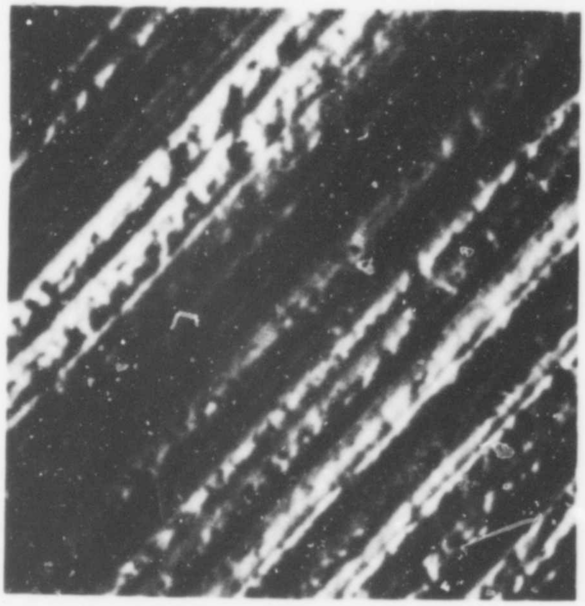

Appearance of Ground
Si_3N_4 Plate. 1000X

AL74P009

ENCLOSURE 43

SURFACE MEASUREMENTS ON GROUND SILICON NITRIDE PLATE

Angular Location	Slope Angle Meter Rdgs. RMS Angle Measurements in Deg. ($\sqrt{m_{20}}$)	C.L.A. Meter Rdgs. Rdg. Microinches - Repeated 4 Times: 1	2	3	4	Average
15°	3.1	10	10.5	9.5	9.5	9.9
30°	3.45	11.5	13	11	12.5	12.0
45°	3.75	11	11	11	11	11.0
60°	4.05	13	13	11.5	11.5	12.3
75°	4.15	13	14.5	15.5	13.5	14.1
90°	4.3	15	14	15	13.5	14.4
105°	4.25	13	11.5	12	12.5	12.3
120°	4.0	13.5	12.5	13	11.5	12.6
135°	3.8	13.5	12.5	13.5	12	12.9
150°	3.55	14.5	14	13	13.5	13.8
165°	2.9	13	13	12.5	13	12.9

ENCLOSURE 44

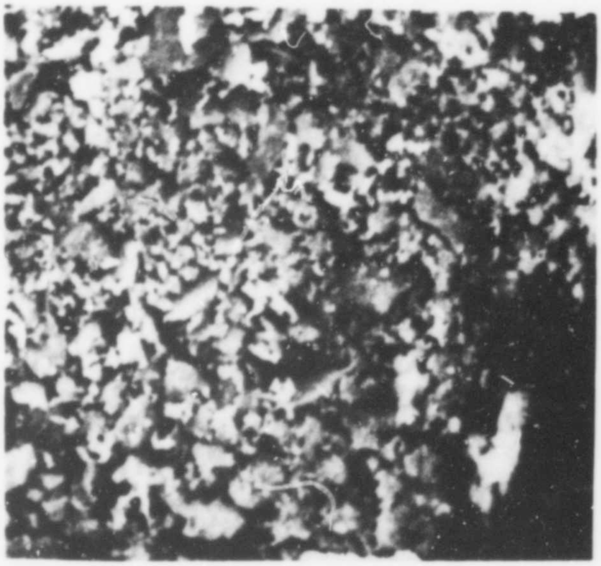

SEM Photograph of Wear
Debris Obtained from
Lap-master Wear Tests
3000X